UNIVERSITAT POLITÈCNICA DE CATALUNYA
BARCELONATECH
Escola d'Enginyeria de Barcelona Est

MASTER'S THESIS

Materials Science and Engineering

DEVELOPMENT OF AN ALGINATE-BASED HYDROGEL LOADED WITH MULTIFUNCTIONAL GOLD NANOPARTICLES FOR REGENERATIVE THERAPIES

Report

Author: Marta Sáez Ríos
Director: Carles Mas Moruno
Co-Director: José Manuel García Torres

Semester: February 2019

Abstract

The aim of this project was to develop a multifunctional alginate-based hydrogel modified with peptide-functionalized gold nanoparticles (AuNPs). Hydrogels are versatile materials, commonly used in tissue engineering due to their biocompatibility and tunable properties. In detail, this project explored the modification of alginate hydrogels with functionalized AuNPs incorporating bioactive peptides, such as LF1-11 or RGD, which are known for preventing bacterial infection and promoting cell adhesion, respectively. To this end, this project focused on the synthesis of AuNPs, their conjugation with peptides and, finally, the hybrid hydrogel preparation. In order to optimize and characterize the fabrication process, several physicochemical techniques were used such as UV-visible spectroscopy, transmission electron microscopy or X-ray photoelectron spectroscopy. The synthesis of the hybrid biomaterial was successfully executed and optimized at each step. The fabrication of this hybrid hydrogel proved to be a robust procedure and highly reproducible. Interestingly, the presence of the antimicrobial peptide LF1-11 decreased the adhesion of bacteria to the hydrogel. Further bacterial and cellular assays are thus warranted in order to ascertain the potential applications of this new biomaterial, e.g. as a film/dressing for infected and chronic wounds or injectable gel for bone defects.

Acknowledgements

First and foremost, I would like to deeply thank the director of this project, Dr. Carles Mas Moruno, and the co-director, Dr. José Manuel García Torres, for their involvement with the project, their constant availability and their helpful advice guiding me throughout this exciting journey.

I would also like to express my gratitude to Dra Joanna M. Sadowska for her kindness helping me with the bacterial assays and the long sessions with the confocal microscope.

I would like to thank as well Trifon Trifonov for his advice in sample preparation and his patience characterizing the gold nanoparticles and the hybrid hydrogels using UV-visible spectroscopy and scanning transmission electron microscopy.

Finally, I also wish to extend my thanks to all the people related to BBT group for helping me in the laboratory.

Glossary

AuNPs – Gold nanoparticles

CF – Carboxyfluorescein

CLSM – Confocal Laser Scanning Microscopy

FTIR-ATR – Fourier transform infrared – attenuated total reflectance spectroscopy

LF – Lactoferrin

NP – Nanoparticle

PBS – Phosphate buffered saline

RGD – Arginine–glycine–aspartic acid peptide

SEM – Scanning Electron Microscopy

SPB – Surface Plasmon Band

SPR – Surface Plasmon Resonance

STEM – Scanning Transmission Electron Microscopy

TEM – Transmission Electron Microscopy

XPS – X-ray Photoelectron Spectroscopy

Table of content

1. Introduction

Biomaterials can be considered as one of the most challenging multidisciplinary fields of research nowadays. In brief, biomaterials are defined as synthetic or natural substances engineered to interact with a living system and obtain a desired therapeutic response. Although biomaterials were originally designed to minimize the response elicited by host tissues after implantation (i.e. they were biocompatible but bio-inert), the field has evolved towards bio-active materials with the capacity to guide complex biological processes. Thus, biomaterials are not regarded merely as supporting scaffolds anymore.

This project will focus on a novel hybrid hydrogel-nanoparticle-peptide composite material that combines unique antibacterial and cell adhesive properties. Such system has potential to produce a new generation of multifunctional films or injectable gels, which may find application for several medical targets, including infected wounds, burns and ulcers.

1.1 Motivation

The motivation of this project is the development of an innovative multifunctional hybrid hydrogel, as a preliminary model for testing their potential applications for regenerative medicine. The combination of a hydrogel with nanoparticles provides the composite material with a versatility that could make it suitable for applications as diverse as topic films, injectable filling for bone defects or 3-D printed scaffolds for tissue engineering. The presence of nanoparticles could be advantageous for conceiving multipurpose materials due to their capacity to be coated, their electrical properties or even inherent antibacterial properties.

Additionally, due to the ease with which nanoparticles can be modified, the incentive of integrating the multifunctional coating developed by the group of Biomaterials, Biomechanics and Tissue Engineering (BBT), which shows successful results for titanium implants. By anchoring a peptide-based chemical platform to the titanium surface, they improved cell adhesion while minimizing bacterial infection (Hoyos-Nogués *et al.*, 2017, 2018). The incorporation of this coating to the novel hydrogel-based support could give rise to promising applications beyond dentistry or orthopedics, with the capacity to produce e.g. films or membranes.

2. State of the art

2.1. Hydrogels

Hydrogels are commonly used in tissue engineering due to their inherent properties and their tunability. They are 3-D cross-linked polymeric networks presenting the peculiarity of absorbing an important amount of water or biological fluids, thus changing their size significantly.

These water-swollen polymers are emerging as a promising tool for cell culture systems since they represent more accurately the characteristics of native tissues than other substrates, e. g. glass substrates, elastomeric films or hydroxyapatite ceramics (Caliari and Burdick, 2016).

The potential applications of hydrogels in tissue engineering rely on their ability to mimic several features of the extracellular matrix, making them favorable for cell hosting. They also have similar mechanical properties to those of soft tissues. As well as, having similar diffusion properties for nutrient and waste exchange, as cell structural support. They are compliant and permeable structures, whose mechanical properties and bioactivity can be easily modified to suit the requirements in order to create not just a physical but also a chemically favorable environment (Bidarra, Barrias and Granja, 2014).

Hydrogels are ideal candidates to be used as wound dressing, as space filling supports, as delivery vehicles for bioactive substances, or as 3-D scaffolds for cell-organization that promote the development of a tissue. The main requisite of hydrogels is their biocompatibility, referred to the ability of being in contact with body organs without compromising the integrity of the surrounding tissues and without triggering undesired responses (Caló and Khutoryanskiy, 2015).

In order to obtain the characteristic 3-D network of hydrogels, and thus the abovementioned properties that differentiate them from other polymeric families, it is necessary the crosslinking of the polymeric chains. Hydrogel formation involves the transition from a liquid viscous precursor solution to the final gelled material. This step can be achieved via physical (noncovalent) or chemical (covalent) methods, such as ionic crosslinking or photocrosslinking. Interestingly for biomedical applications, it can be done under mild conditions for certain hydrogels (Caliari and Burdick, 2016).

Hydrogels can be classified as natural or synthetic, depending on the source employed to synthesize them. Hereunder, we are going to review those which have relevance in the biomedical field.

Natural polymers have highly interest due to their inherent biocompatibility, low toxicity and biodegradability. There are two main types, polysaccharides and fibrous proteins. They are both components of the extracellular matrix. The most common ones are chitosan, alginate, and collagen.

Chitosan and alginate are both polysaccharides. They are non-toxic, stable, and biodegradable that can be sterilized. Alginate is hydrophilic and can be easily crosslinked under mild conditions using divalent or trivalent cations, making it a very convenient candidate. However, unmodified chitosan is not soluble at neutral pH, thus it cannot be used as an injectable hydrogel. Collagen is a protein-based polymer, from which gelatin is extracted by partial hydrolysis, present in connective tissue such as skin, bone, cartilage, and tendons. They present excellent biocompatibility and biodegradability, though it can be affected when increasing the hydrogel stiffness by chemical crosslinking (Heo *et al.*, 2014; Hunt *et al.*, 2014; Caliari and Burdick, 2016)

On the other hand, in spite of having controllable physical properties, synthetic hydrogels lack biological stimuli, thus modification is required to promote cell-material interaction. The most widely used are poly(ethylene glycol) (PEG), poly-(NIPAAM), poly(vinyl alcohol) (PVA), poly(propylene fumarate) (PPF), and poly(hydroxyethyl methacrylate) (PHEMA). They all need to be modified by conjugation with biological factors, such as peptides or polysaccharides (Hunt *et al.*, 2014).

2.1.1. Alginate

Alginate is the main polysaccharide found in brown seaweeds, which consists of a linear block copolymer of D-mannuronic (M) and L-guluronic (G) acid, as schematized in Figure 2.1. These units are randomly arranged along the chain in different proportions, thus different types of alginic acid are obtained depending on the source.

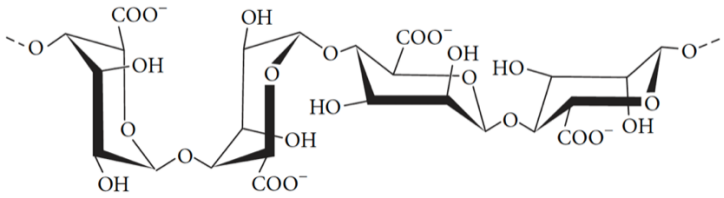

Figure 2.1 Idealized structures of the chemical units of alginic acid (Pereira, Gheda and Ribeiro-Claro, 2013).

The main interest of alginate is its simplicity to form hydrogels under mild conditions via ionic crosslinking. The addition of divalent cations such as Ca^{2+}, Mg^{2+} or Ba^{2+} promotes the formation of ionic bridges between G units, as represented in Figure 2.2. It can be formed in situ in aqueous solution, using non-toxic solvents and under physiological conditions (Caliari and Burdick, 2016).

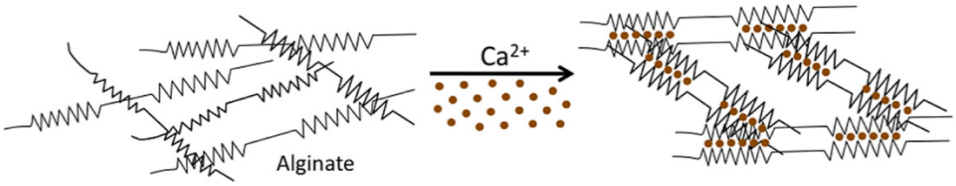

Figure 2.2 Alginate hydrogel formation by ionic crosslinking (Bidarra, Barrias and Granja, 2014).

Tailored alginates have been developed for different applications, including their use as tissue bulking agents, as controlled drug delivery systems, or as cell delivery vehicles in tissue engineering. Coupled with its advantageous preparation, alginate presents multiple benefits for biomedical applications, the most relevant being non-immunogenicity, biocompatibility and non-toxicity (Augst, Kong and Mooney, 2006).

Moreover, alginate mechanical properties can be adjusted by changing polymer source, molecular weight, and/or type and density of crosslinking. Thus, the stiffness can be modified to better mimic a tissue, tuning the compression modulus within the range 1 to 1000 kPa and the shear modulus from 0.02 to 40 kPa (Bidarra, Barrias and Granja, 2014).

However, alginate shows two major drawbacks. On the one hand, it slowly degrades in the presence of counterions, where Ca^{2+} is exchanged by non-gelling monovalent ions (e.g. Na^{+}) producing de-crosslinking. Therefore, alginate stability depends on the physiological conditions (Bidarra, Barrias and Granja, 2014). On the other hand, alginate is not a bioactive polymer requiring its modification to enable cell interaction (Caliari and Burdick, 2016).

The chemical versatility of alginate allows the easy integration of biochemical cues to cause specific cell responses. One of the most common methods to promote cell attachment to alginate is the incorporation of cell recognition motifs, such as RGD, as it has been demonstrated in several studies (Figure 2.3). The arginine–glycine–aspartic acid (RGD) peptide sequence promotes cell adhesion. It corresponds to the minimal essential cell adhesion peptide sequence identified in several proteins present in the extracellular matrix, which are associated with integrins in cell surface membranes. The functionalization of alginate with RGD is done through a stable covalent amide bond between the carboxyl group of alginate and the N-terminus of the peptide (Bidarra, Barrias and Granja, 2014).

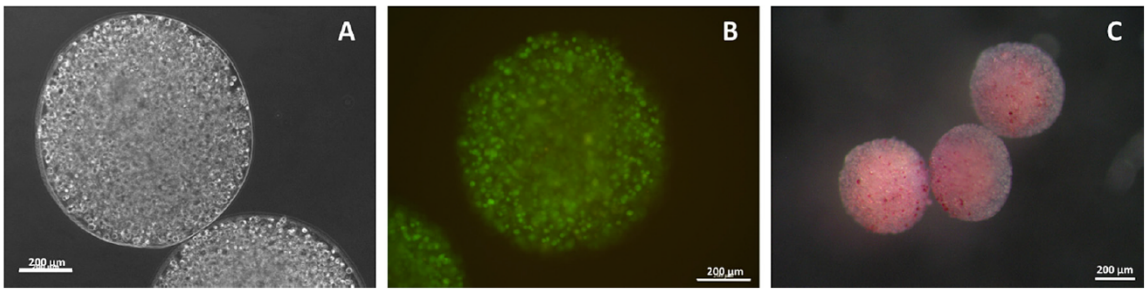

Figure 2.3 Osteogenic differentiation of human mesenchymal stem cells (hMSCs) inside alginate hydrogel microspheres: (A) hMSCs within 2 wt.% RGD–alginate microspheres remain with a high viability after 21 days in culture, (B) as demonstrated by the Live/Dead assay (viable cells stain Green), (C) express high levels of alkaline phosphate activity (ALP) (a common osteogenic marker, ALP+cells stain pink) (Bidarra, Barrias and Granja, 2014).

2.2. Hybrid hydrogels

It is clear the potential applications of hydrogels, due to their capacity to mimic different features of the extracellular matrix. However, even natural hydrogels require modifications either to improve their physical properties or to increase their bioactivity. Two strategies are usually followed to improve the hydrogel characteristics, one being the direct functionalization of the hydrogel with a peptide sequence, as demonstrated for alginate in section 2.1.1, the other one being the incorporation of inorganic nanoparticles, as it will be further discussed in this section.

The peptide functionalization of alginate benefits cell attachment. Nevertheless, hydrogels do not possess bactericidal properties. Bacteria can potentially attach to the surface of hydrated polymeric matrix and aggregates, creating biofilms. The main concern nowadays is the increasing resistance of bacteria to antibacterial drugs. It is derived then that the interest is not only promoting cell adhesion but also synthesizing hydrogels with bactericidal properties. The most promising approach is the addition of metal nanoparticles within the hydrogel matrix, that have already been proved effective to combat bacteria like silver nanoparticles (González-Sánchez *et al.*, 2015). Hybrid hydrogels combine the benefits of polymers and nanoparticles. Further applications could be developed taking advantage of the incorporation of metallic nanoparticles, in terms of hydrogels with electrical or magnetic properties.

2.2.1. Metallic nanoparticles

Nobel metals present drastically different properties in the nanoscale, compared to the bulk material. Nanoparticles (NPs) have at least one dimension less than 100 nm. Their main characteristic is the

increase of specific surface compared to the bulk material. In the nanoscale, many physicochemical properties are size-dependent, such as the optical and electronic properties due to quantum size effect. They can also present magnetic properties due to the uneven electronic distribution. Additionally, being in the solid state, they present higher thermal conductivity than solid fluids (Morais *et al.*, 2013).

Nanotechnology is lately extending its applications within the biomedical field by implementing the use of NPs. Different types of NPs have been used for imaging, biosensing, drug delivery system or cancer diagnostics, due to their optical and electronic properties. For these applications, NPs smaller than 100 nm are able to interact with the biological target of interest. NPs must be nontoxic, biocompatible and stable in biological media. Another advantage is that they can be functionalized in order to increase their bioactivity. For biomedical applications, the main metallic NPs studied are gold (AuNPs) and silver (AgNPs) due to their broad-spectrum antimicrobial activity (Kogan *et al.*, 2007).

AgNPs are a strong antiseptic, present minimal toxicity issues and lower the incidence of inflammation. Silver has always been known for their effectiveness combating bacteria. However, late studies demonstrate that bacteria are developing resistance to AgNPs antibiotic activity (Drabczyk *et al.*, 2017). Moreover, AgNPs can also be toxic for eukaryotic cells (Mei *et al.*, 2014).

AuNPs are reemerging as a lead candidate in nanoscience thanks to their simple synthesis and their controllable size from 0.8 to 200 nm. They can be easily conjugated with different biological molecules and present excellent biocompatibility and stability. Moreover, AuNPs possess unique optical properties simplifying its characterization (Sonavane, Tomoda and Makino, 2008).

Additionally, it has been stated in the literature that AuNPs promote osteogenic differentiation of mesenchymal stem cells (MSCs). In the study of Heo *et al.*, 2014, a hybrid gelatin-based hydrogel with AuNPs causes the same regeneration effect as bone morphogenic proteins (BMP-2). Bone defects were created and filled with different types of hydrogels (non-loaded, loaded with BMP and loaded with different concentrations of AuNPs). The results, summarized in Figure 2.4, show that all of them promote bone healing compared to the control group. Particularly, the AuNPs-loaded hydrogel presented improved bone regeneration for longer time and higher concentration. Furthermore, AuNPs do not present the disadvantages of BMP-2 of expensiveness and unwanted bone formation, since it is a very strong osteoinductive protein.

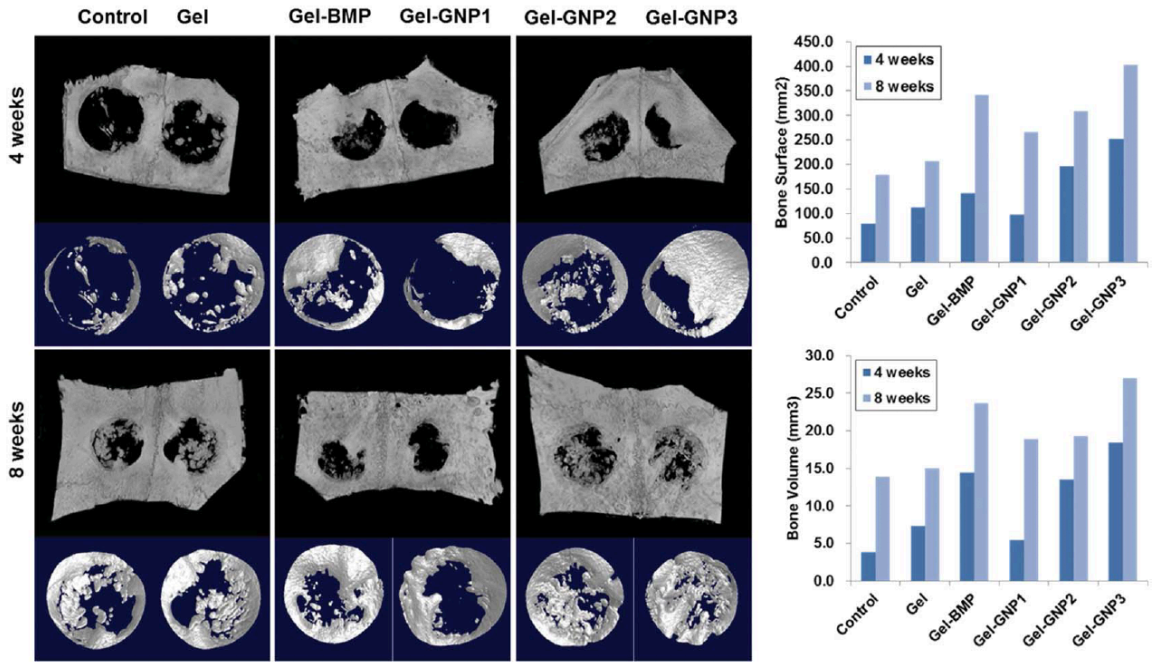

Figure 2.4 3-Dimensional scan images of rabbit calvaria after 4 and 8 weeks of implantation, and recovered bone area of the defected sites (Heo *et al.*, 2014).

Despite being biochemically inert and biocompatible in bulk size, the behavior of gold and silver in the nanoscale is completely different. In fact, as mentioned above, a general awareness of potential nanoparticle toxicity is being raised, especially regarding silver. Conflicting data concerning the cytotoxicity of NPs is available in the literature. Nevertheless, it is agreed that NP toxicity is directly related to its dimensions. The potential toxicity is determined by the ability of a NP to cross cell membranes (cell size 10-100 μm), thus to its dimensions. In the case of gold, they can be considered nontoxic for sizes above 15 nm (Marsich *et al.*, 2011).

2.3. Functionalization of biomaterials

In order to exploit the potential applications of hybrid hydrogels, and all biomaterials in general, it is advisable to functionalize them with proteins or peptide sequences to increase their bioactivity, and thus their overall performance.

RGD is the most common ligand that promotes cell adhesion, as mentioned in section 2.1.1. To go a step further and also prevent biofilm formation, Hoyos-Nogués *et al.*, 2017 proposed a multifunctional tailor-made peptide-based chemical platform whose chemical structure is shown in Figure 2.5. This branched structure incorporates the RGD sequence in one branch, and the lactoferrin-derived LF1-11 in the other one. LF1-11 is an antibacterial peptide that acts by interacting and perturbing both Gram-

negative and Gram-positive membranes. This promising multifunctional strategy has been proved to work on titanium surfaces by improving osteoblast differentiation and inhibiting early bacterial adhesion of *S. sanguinis* and *S. aureus* and reducing biofilm formation.

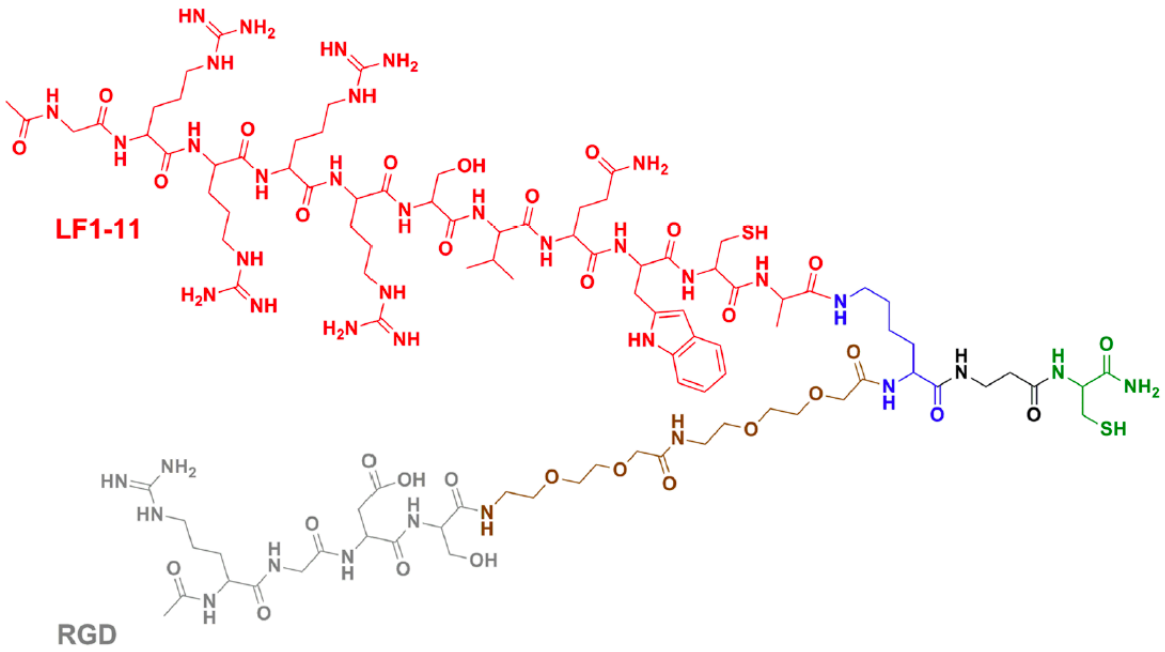

Figure 2.5 Multifunctional platform (in brown spacer, in blue branching unit, in green anchor group) (Hoyos-Nogués *et al.*, 2017)

3. Objectives of the project

This project aims to fabricate and characterize a new family of composite materials based on alginate hydrogels incorporating gold nanoparticles functionalized with peptide sequences that can provide the biomaterial with antibacterial and/or cell adhesive properties.

The main objective is to stablish a methodology for fabricating this novel material, in order to make it reproduceable for testing its potential applications, such as multifunctional films or injectable gels. To optimize this process, several characterization techniques will be required.

Keeping in mind the composite nature of this biomaterial, which is a hydrogel-nanoparticle-peptide combination, the specific objectives of this project are:

1. Synthesis of AuNPs.
2. Functionalization of the AuNPs with peptide.
3. Fabrication of alginate hydrogels incorporating the functionalized AuNPs.

Ultimately, this project aims to incorporate the peptide platform designed by BBT, which shows both antibacterial and cell adhesion properties, in order to produce a new generation of versatile multifunctional biomaterials and spread the applicability of such peptide platform toward new targets.

3.1. Extension of the project

The extension of this process includes initially the bibliographic research of hydrogel-based biomaterials that can be valid candidates for the peptide incorporation, designing an optimized methodology to prepare it by the means available, and its thorough characterization at each step, using the most suitable techniques for hydrogels.

3.2. Project development

This project involves three well differentiated stages considering the composite nature of the biomaterial, as it is schematized in Figure 3.1. First and foremost, the synthesis of AuNPs and their characterization in order to verify their size and composition. Secondly, the conjugation of these AuNPs with the peptide sequences of interest for later biological assays, and their characterization to ensure the peptide attachment to gold surface. Afterwards, the incorporation of the functionalized AuNPs into a hydrogel matrix and the physicochemical characterization of this novel biomaterial to confirm the

AuNPs presence. Finally, biological assays will be carried out with the hybrid hydrogel to examine its interaction with living systems.

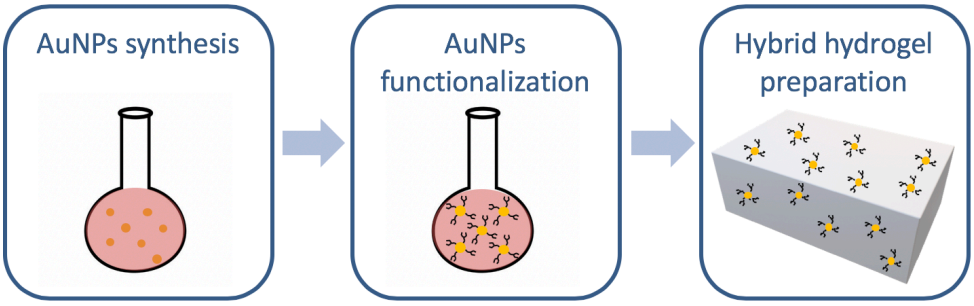

Figure 3.1 Schematic representation of the three main stages of the development of the hybrid hydrogel.

4. Experimental section

4.1. Synthesis of AuNPs

The synthesis of AuNPs was performed following the Turkevich method, a well-known method developed by J. Turkevich in 1951. The obtainment of a monodisperse gold suspension is done by chemical reduction of a metallic salt. Tetrachloroauric acid ($HAuCl_4$) is reduced in aqueous solution using sodium citrate (Na_3Ct) at 100°C, as shown in Figure 4.1. Sodium citrate acts as both reducing and capping agent, helping to stabilize the gold particles.

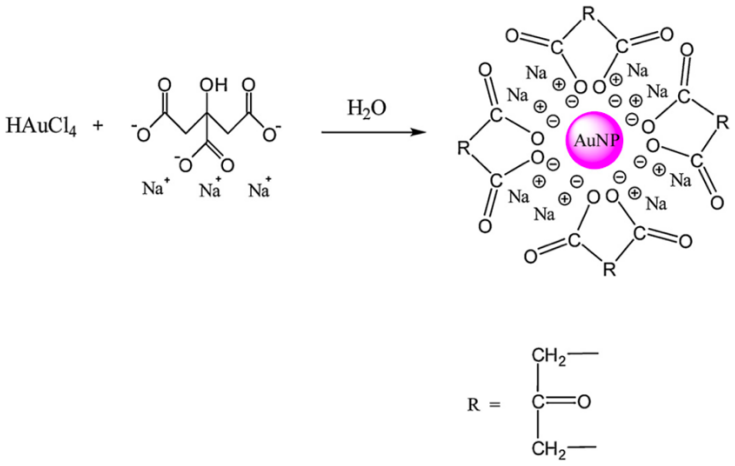

Figure 4.1 AuNPs synthesis following the Turkevich method (Zhao, Li and Astruc, 2013).

The Turkevich method is widely used due to its simplicity and the possibility to control the final particle size. It is a seed-mediated growth mechanism where the number of nanoparticles is defined at the initial stage of the synthesis and remains constant during the reaction. Thus, the particle size depends on the citrate-to-gold ratio. The initial concentration of $HAuCl_4$ has important influence during the seed particle formation. For higher $HAuCl_4$ concentrations, more seeds are formed; therefore, smaller gold particles are obtained (Wuithschick *et al.*, 2015).

To perform the synthesis of 16 nm AuNPs, 10 mg of tetrachloroauric acid ($HAuCl_4$, Sigma Aldrich (254169)) was added to 100 mL of Milli-Q water and the solution was heated to boiling under reflux, as shown in Figure 4.2. Then, 3 mL of warm 1% sodium citrate (Na_3Ct, Sigma Aldrich (25114)) solution were added to the previous solution under vigorous stirring. Samples at 10, 30 and 60 min were taken to characterize the evolution of particle size with time. The initial colorless gold solution changed to the characteristic red wine color of spherical AuNPs, as shown in Figure 4.3 (Avvakumova *et al.*, 2014).

The citrate-to-gold ratio is expressed using the concentration in the final aqueous solution, [$HAuCl_4$] = 0.29 mM and [Na_3Ct] = 3.76 mM.

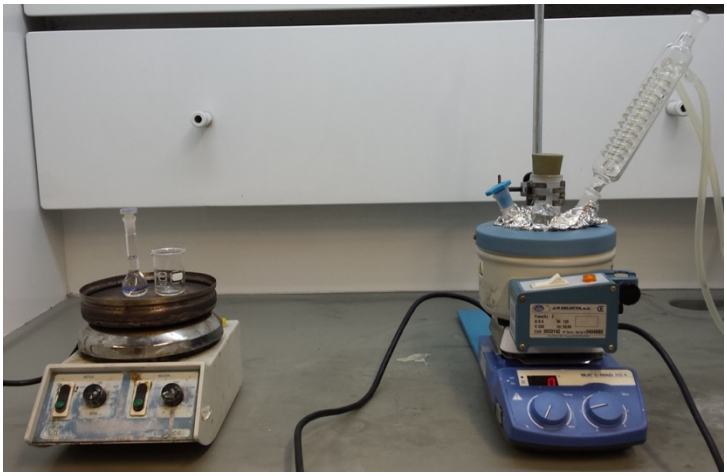

Figure 4.2 Experimental setup for the synthesis of AuNPs.

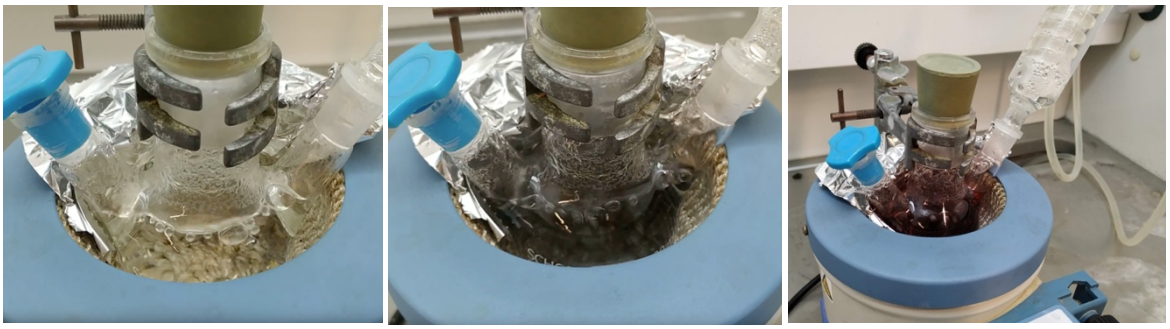

Figure 4.3 Characteristic color change during AuNPs formation, after addition of sodium citrate.

4.2. Characterization of AuNPs

Taking advantage of the unique optical properties of AuNPs, UV-vis spectroscopy is a simple technique that can be used to characterize them. At the nanoscale, gold colloidal solutions present bright colors (red or purple), not a gold color as the bulk material. The reason is the interaction of light, at specific wavelengths, with the electrons on the nanoparticle surface. This produces a collective oscillation of the electrons in the conduction band, known as surface plasmon resonance (SPR), responsible of the characteristic red color of the AuNPs solutions (Murphy *et al.*, 2008). The SPR produces an extinction spectrum dependent on the AuNPs size, shape and agglomeration state. For AuNPs aqueous solutions, a broad absorption band appears in the extinction spectra in the visible region around 520 nm. The

surface plasmon band (SPB) is absent for AuNPs with a diameter below 2 nm and for bulk gold. (Astruc and Daniel, 2004).

The UV-vis spectrophotometer used to record the spectra Shimadzu 3600. No sample preparation is required for UV-vis spectroscopy. The accessory of cuvettes is used to analyze straightaway the AuNPs solutions. The spectra were obtained over the wavelength range from 300 to 800 nm.

Transmission Electron Microscopy (TEM) is the most frequently used technique to obtain images to calculate NPs size distribution due to its easy sample preparation. TEM images were initially taken, however because of technical problems with the equipment, Scanning Transmission Electron Microscopy (STEM) was used for the same purpose. The working principle is the same, using electron-transparent samples the transmitted electrons are analyzed to obtain brightfield images. The difference is that in STEM the electron beam scans the sample, while in TEM the beam is static. Samples must be electrically conductive, therefore a drop of 20 μL of AuNPs solution was deposited over a carbon-coated copper grid and left to evaporate. The samples were analyzed in the using the Focused Ion Beam Zeiss Neon40 equipment.

4.3. Functionalization of AuNPs

The aim of modifying the surface of AuNPs with biomolecules is to increase their functionality and biological properties. Citrate, which stabilizes the AuNPs during their formation through noncovalent interactions, can be easily displaced by other species with higher binding affinity as shown in Figure 4.4. Thiol groups present high affinity to gold, so they are commonly used to conjugate active groups such as peptides (Yeh, Creran and Rotello, 2012).

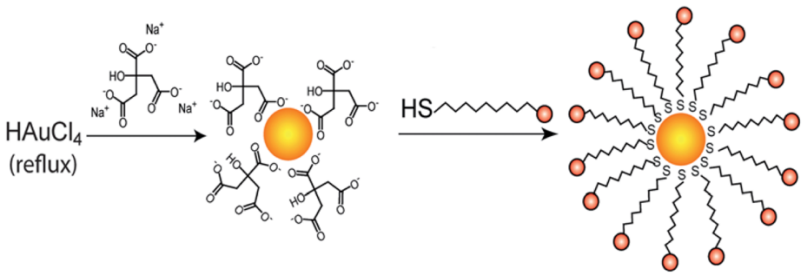

Figure 4.4 Ligand exchange of functionalized thiols for citrate-stabilized AuNPs (Adapted from *Yeh, Creran, and Rotello 2012)*.

In this project the biomolecule conjugated to the AuNPs is the peptide-based platform shown in Figure 4.5, which presents two bioactive sequences, LF1-11 and RGD. It is the same molecule previously explained in section 2.3.

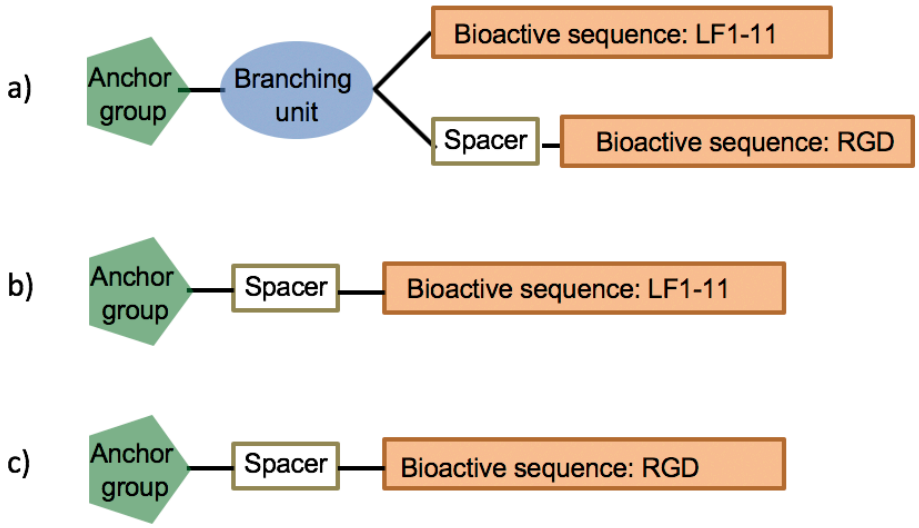

Figure 4.5 Schematic representation of the peptide conjugates (a) multifunctional branched peptide platform containing both LF1-11 and RGD, (b) linear peptide containing LF1-11, and (c) linear peptide containing RGD.

The synthesis of this platform is costly and the quantity available of molecule was thus limited. Therefore, to optimize the conditions of peptide conjugation and incorporation into hydrogels, control linear peptides (either RGD or LF1-11) were used instead. They were provided by the Biomaterials, Biomechanics and Tissue Engineering (BBT) research group and were produced by solid-phase peptide synthesis (SPPS). The linear peptide sequences used were: SH-RGD and SH-LF1-11, as schematized in Figure 4.5 (a), (b). In addition, a fluorescently-labelled SH-RGD-CF peptide was used as well. Carboxyfluorescein (CF) is a fluorophore which has been added to our biomolecules to label them and allow further characterization via fluorescence techniques.

The conjugation was performed using an excess of peptide. 1mL of peptide solution (1mg/mL in Milli-Q water) was added dropwise to 10mL of AuNPs solution at room temperature under vigorous magnetic stirring during 15 min (Hosta *et al.*, 2009). Afterwards, the conjugated AuNPs are purified to eliminate the excess peptide by dialysis. A 14 kDa dialysis tubing cellulose membrane (Sigma Aldrich, D9777) is used against a solution of 1 mM sodium citrate. The dialysis is carried out over 24 hours under magnetic agitation and the solution is refreshed three times. The experimental setup is represented in Figure 4.6. In the case of the peptide containing CF, which is a fluorophore light-sensitive, the bath is covered with aluminum foil to protect it from the light.

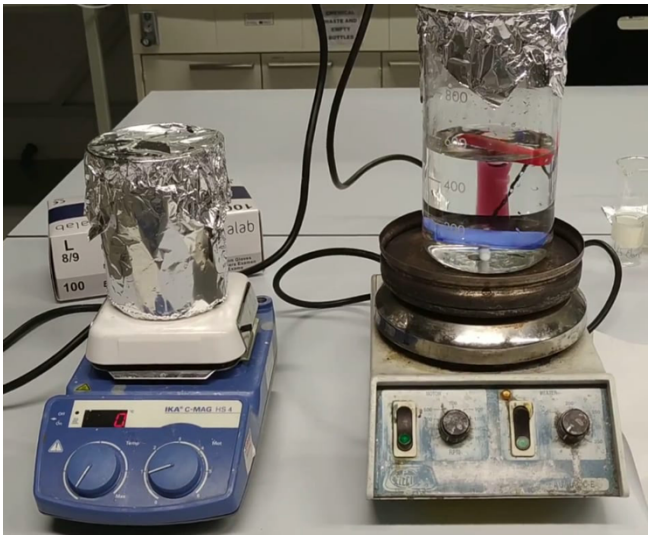

Figure 4.6 Experimental setup for the dialysis. On the left dialysis of the peptide containing CF protected from the light and on the right dialysis of SH-RGD peptide.

4.4. Characterization of conjugated AuNPs

As explained in section 4.2, UV-vis spectroscopy is a very useful technique for the estimation of particle size but also for analyzing the functionalization of bare AuNPs. A change in the nanoparticle environment induces a shift of the surface plasmon band due to the ligand shell created by the peptide around the AuNPs, causing an alteration of the refractive index. The spectra were again obtained over the wavelength range from 300 to 800 nm in order to compare it to the bare AuNPs.

The peptide sequences labeled with a fluorophore can be characterized using fluorescence microscopy, such as Confocal Laser Scanning Microscopy (CLSM). This technique, in combination with UV-vis spectroscopy, allows to confirm the presence of peptide recovering the AuNPs surface. Carboxyfluorescein has an absorption wavelength of 495 nm and an emission wavelength of 517 nm. A drop of conjugated AuNPs solution was placed on a glass-bottom Petri dish and left to evaporate. The CLSM equipment used was Carl Zeiss LSM 800 with the objective lens 63x.

4.5. Preparation of alginate films loaded with AuNPs

Alginate hydrogels were prepared by drop casting from 3.4 wt.% alginic acid sodium salt (Panreac) solution. Different samples were prepared in order to compare the effect of incorporating the AuNPs into the hydrogel matrix: alginate films without AuNPs, alginate films with non-functionalized AuNPs

and alginate films with functionalized AuNPs (RGD or LF1-11). Films with two different amounts of the functionalized and non-functionalized AuNPs were prepared.

As alginate is a water-soluble polysaccharide, distilled water was used to prepare the alginic acid solution. When AuNPs-containing hydrogels were prepared, the distilled water was replaced by the AuNPs solution. (after dialysis) The AuNPs solution was sonicated before use because agglomeration was noticed during storage. A probe sonicator (Branson Digital Sonifier) was employed at 20% amplitude over 1 min in pulse mode (pulse ON=1 s, pulse OFF =1 s). Table 4.1 summarizes the content of all the components (alginate, water and AUNPs solution) to prepare the aforementioned hydrogels. The solution was manually mixed in a beaker using a spatula by slowly addition of the alginate powder to minimize the formation of lumps. Then, to obtain a homogeneous solution without bubbles, they were introduced in the SpeedMixer^{TM} (DAC 150.1 FVZ) for 5 min at 3500 rpm.

Table 4.1 Preparation of 3.4 wt.% alginate-based films.

FILM	$m_{alginate}$ (g)	$V_{distilled\ water}$ (mL)	$V_{AuNPs\ solution}$ (mL)
Alginate	0.170	5	0
Alg + AuNPs 3mL	0.170	2	3
Alg + AuNPs 5mL	0.170	0	5
Alg + conjugated AuNPs 3mL	0.170	2	3
Alg + conjugated AuNPs 5mL	0.170	0	5

The films were prepared by drop casting a given mass (0.3 g) of the solution onto a microscope slide, as shown in Figure 4.7. The area (2x2 cm) was controlled in order to have films with comparable thicknesses. The solution was gently casted onto the substrate to avoid the formation of bubbles. The sample was left to rest during 30 min to ensure a homogenous distribution.

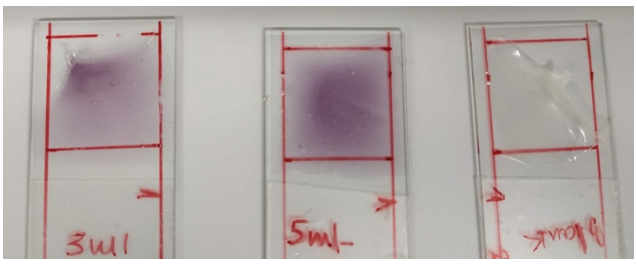

Figure 4.7 Final hybrid hydrogels after being crosslinked and left to dry overnight.

Afterwards, the crosslinking of the polymer chains to acquire the characteristic 3-D structure of hydrogels was done adding 0.1 M calcium chloride ($CaCl_2$, Sigma Aldrich) solution. The ionic crosslinking provides the material with the hydrogel properties. To perform this step, the samples were introduced in calcium chloride baths, making sure they were completely covered, over 2 hours to guarantee a completely diffusion of the Ca^{2+}.

4.6. Characterization of alginate films loaded with conjugated AuNPs

The composite hydrogels were characterized using multiple techniques to determine the presence of the conjugated AuNPs within the hydrogel matrix, their distribution and their biological activity. Different sample preparation is required depending on the technique.

First and foremost, UV-vis spectroscopy was also used to determine the presence of AuNPs within the hydrogel. However, in this case, an accessory for solid samples is used, instead of the cuvettes. The films prepared were left to dry overnight after the crosslinking step in order to remove the excess of water.

STEM was used to detect and characterize the distribution of AuNPs within the hydrogel. The samples were dried, fixed onto the stub using conductive adhesive tape and coated with carbon to make them electrically conductive.

Fourier transform infrared – attenuated total reflectance (FTIR-ATR) spectroscopy is a reliable technique for fingerprinting many materials. It allows the identification of functional groups, so in our case the presence of characteristic groups that form alginate and the peptide sequences. An infrared beam is sent to an optically dense crystal with a high refractive index, typically germanium. The internal reflection of the beam creates an evanescent wave that transmits into the sample in direct contact with the crystal. The variations in the infrared spectrum are a result of the different absorption energies of the sample at different IR regions that attenuate the evanescent wave. For the present case study, the spectra are obtained within the wavelength range 4000 – 800 cm^{-1} using the FTIR Nicolet 6700.

X-Ray Photoelectron Spectroscopy (XPS) gives quantitative information about the elements present in a sample provided by the binding energy. The chemical composition (atomic %) of the biomaterials was analyzed using a non-monochromatic Mg anode X50 source (150 W) and a Phoibos 150 MCD-9 detector (D8 advance, SPECS Surface Nano Analysis GmbH). Detector pass energy was fixed at 25 eV with 0.1 eV steps to record high resolution spectra at a pressure below 7.5×10^{-9} mbar. The elements of the high-resolution analysis were C, N, O, S and Au, with binding energies referenced to a fixed C1s signal (284.8 eV). The spectra were analyzed using Casa XPS software. The samples were analyzed in duplicate.

In order to analyze the biological response of the hybrid hydrogel, a bacterial viability Live/Dead assay was performed. In this case, to test the antibacterial properties the hybrid hydrogel used was the one containing the LF1-11-conjugated AuNPs, which is the antibacterial peptide sequence.

An adaptation from Hoyos-Nogués *et al.*, 2017 protocol was used, bearing in mind the 3-D structure of hydrogels and their swelling ability. The assay is performed in static conditions and using two replicates for each condition. The bacteria used was *S. aureus,* which is associated to implant infections. It was inoculated overnight at 37ºC in Heart Infusion Broth (BHI). A bacterial suspension was prepared at a bacterial concentration of 10^8 colony forming unit (CFU)/mL. The hydrogel samples were cut into small disks to fit in 24-well plates and sterilized with ethanol 70% (v/v) during 30 min. Samples were washed three times with PBS and incubated with 50 μL of bacterial suspension for 4 h at 37ºC. After this, the samples were changed to a new 24-well plate and washed 3 times with PBS, as shown in Figure 4.8. In the case of the negative control samples, they were washed with Triton100 0.1% solution (v/v) with PBS. Then, bacteria were fixed using 0.5 mL of glutaraldehyde solution 2.5 % (v/v) (Sigma Aldrich) with PBS over 30 min in the fridge. Samples were washed with PBS over 30 min. Finally, the samples were incubated during 3 min in the dark with 10 μL of a solution containing two dyes for fluorescence spectroscopy observation. The dyes solution was prepared by adding 3 μL of SYTO and 3 μL of propidium iodide to 2 mL of PBS buffer, from the LIVE/DEAD™ BacLight™ Bacterial Viability Kit (ThermoFisher). SYTO 9 is a green-fluorescent nucleic acid that stains all bacterial cells, whereas propidium iodide is a red-fluorescent nucleic acid that only penetrates damaged cell membranes. Using CLSM, images of the bacteria viability can be examined.

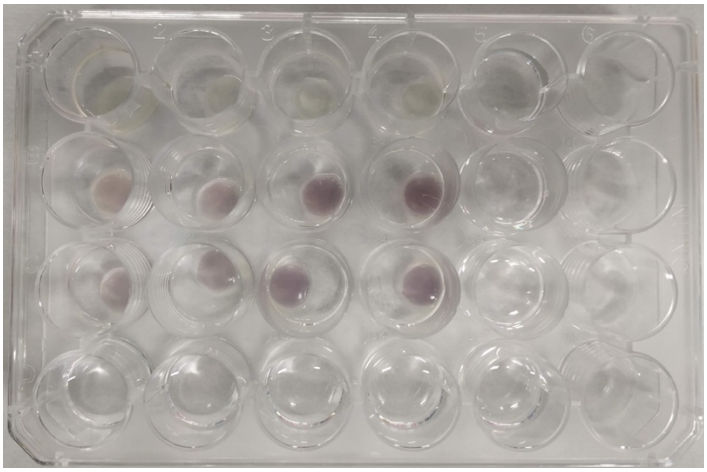

Figure 4.8 Samples in a 24-well plate after 4 h of incubation with *S. aureus*. First row alginate films, second row Alg + AuNPs, third row Alg + AuNPs-LF1-11.

5. Results and discussion

5.1. Characterization of AuNPs

First, AuNPs were synthesized via the sodium citrate reduction method. Despite being a common synthesis method, it was an unknown method by our group. Therefore, different trials of synthesis were necessary before stablishing the optimum experimental conditions.

5.1.1. 1st synthesis

The first synthesis of AuNPs was carried out following the methodology specified by Avvakumova et al. 2014. The reaction was left under reflux during 60 min. An aliquot was extracted after 10 min of adding the sodium citrate solution, as a control, when the solution had already turned into red color.

The UV-vis spectra of both samples in Figure 5.1 present the characteristic absorption band of AuNPs in the visible region around 520 nm (Astruc and Daniel, 2004). A sharp narrow peak centered at 523 nm is observed for the aliquot extracted after 10 min of reaction. However, the 60-min reaction sample presents a wider and lower peak at 526 nm. Shape, size and aggregation of the nanoparticles are generally the variables that affect the optical properties and, consequently, the UV-Vis spectra (Murphy *et al.*, 2008). The broadening of the 60-min peak could be related to a higher particle size or to some extent of aggregation, which are the common causes of a red-shift of the peak. Apparently, a longer reaction time does not seem to ensure the obtainment of a homogenously distributed spherical colloidal solution.

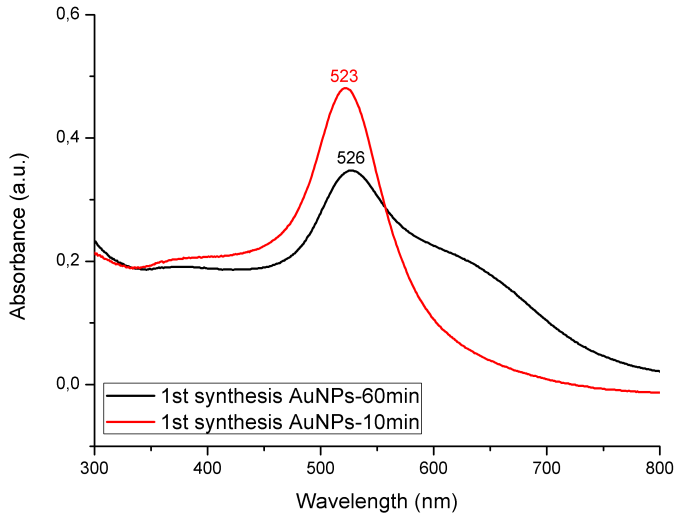

Figure 5.1 UV-vis absorption spectra of the 1st synthesis of AuNPs.

5.1.2. 2nd synthesis

In order to analyze the effects of reaction time on the AuNPs appearance, a second synthesis was carried out. This time samples at 10, 30 and 60 min were collected. The UV-vis spectra in Figure 5.2 shows a sharp absorption band at 521 nm for 10- and 30-min samples, which agrees with the literature (Astruc and Daniel, 2004). Nevertheless, an unexpected spectrum is obtained for the 60-min sample which presents a double peak at 532 and 730 nm. AuNPs spectrum is tightly related to their size and shape. The double peak is often related to irregular-shaped nanoparticles. In spherical AuNPs the plasmon oscillations are isotropic due to the spherical symmetry. However, for irregular AuNPs, such as nanorods, two plasmon bands transversal and longitudinal can be observed, (Murphy *et al.*, 2008). Further analysis via visual techniques such as TEM would be necessary to confirm it.

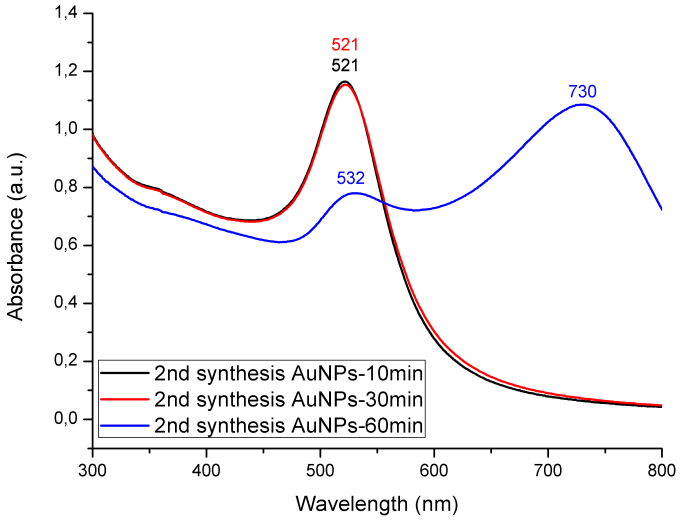

Figure 5.2 UV-vis absorption spectra of the 2nd synthesis of AuNPs.

Figure 5.3 shows a TEM image of the 10-min synthesis. TEM is a more precise technique for evaluating the size and shape of the AuNPs**.** Despite the color change of the solution to red and the sharp peak at 521 nm, there are clearly unreacted salts. Therefore, we can conclude that the synthesis is not completed.

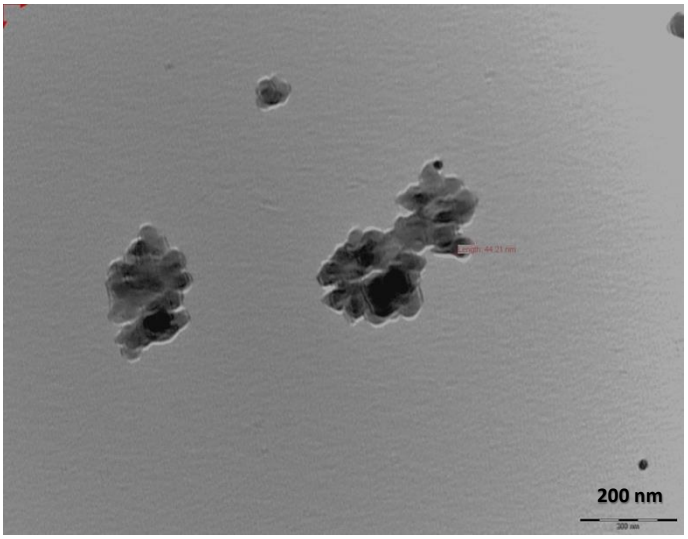

Figure 5.3 TEM image of AuNPs 2nd synthesis 10 min.

On the other hand, the 60-min sample shown in Figure 5.4 does not present unreacted salts. After evaluation of different regions of the sample there were no clear signs of irregular-shaped nanoparticles, such as nanorods, to relate it to the double peak in the UV-vis spectrum. All the AuNPs have more or less a spherical aspect. However, a certain degree of agglomeration could be detected that could explain the spectrum.

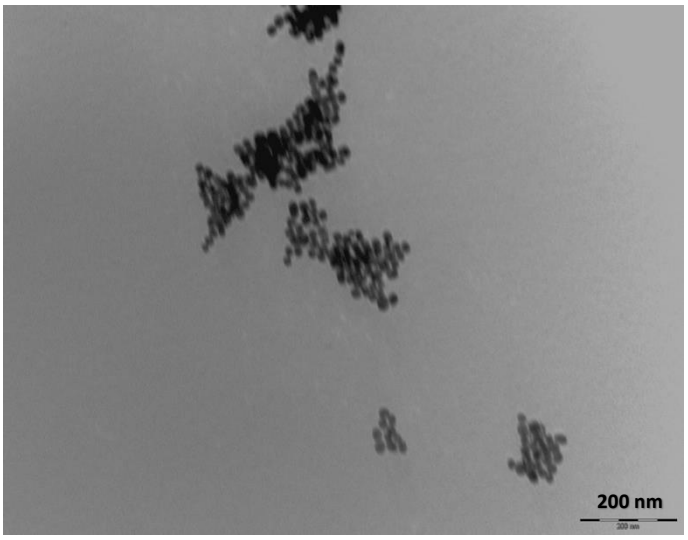

Figure 5.4 TEM image of AuNPs 2nd synthesis 60 min.

5.1.3. 3rd synthesis

After careful consideration of the previous results and some research, a 30-min synthesis was concluded to be the optimal compromise to avoid unreacted salts and prevent aggregation. Thus, a third synthesis was performed under these conditions and the results analyzed.

An absorption band at 522 nm is presented in the UV-Vis spectrum in Figure 5.5, which agrees with the literature (Astruc and Daniel, 2004). From STEM images (Figure 5.6), it is observed that the morphology of AuNPs is generally spherical and that they are almost free of aggregation.

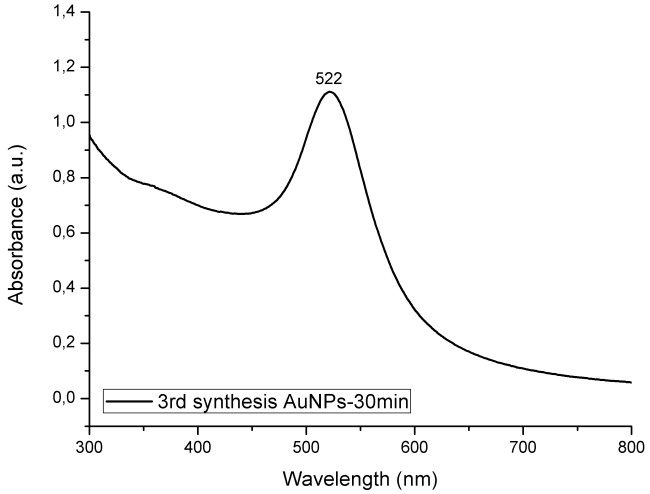

Figure 5.5 UV-vis absorption spectrum of the 3rd synthesis of AuNPs.

Figure 5.6 STEM image of AuNPs 3rd synthesis 30 min.

5.1.4. Nanoparticle size distribution and concentration

The mean nanoparticle diameter was determined analyzing the STEM images of the 3rd synthesis. ImageJ software was used to process the images, the diameter of more than 400 AuNPs was measured and the calculated average diameter is 16.2 $\pm$ 2.5 nm (Figure 5.7), in agreement with the followed article (Avvakumova *et al.*, 2014). As it can be observed, monodisperse spherical particles have been obtained following the synthetic procedure previously explained.

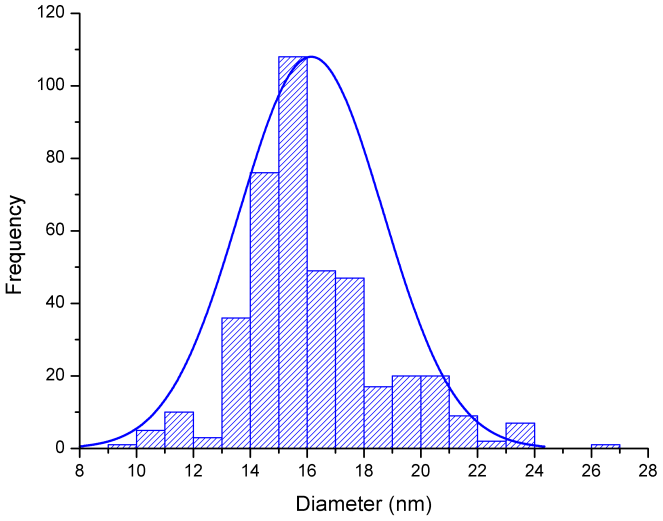

Figure 5.7 Histogram and normal distribution of the measured diameters of over 400 AuNPs.

Another piece of information that can be extracted from the combination of the mean diameter and the UV-Vis spectrum is the concentration of AuNPs. A fast method provided by Haiss, 2007 allows the determination of the concentration (c) of uncoated spherical AuNPs, according to Equation 5.1. The value of the coefficient of extinction (ε_{450}) is tabulated and depends on the nanoparticle diameter. For 16-nm nanoparticles, the tabulated value is $\varepsilon_{450} = 2.67 \cdot 10^8$ M^{-1} cm^{-1}. The absorbance at 450 nm for a standard path length of 1 cm is extracted from the UV-Vis spectrum, which is $A_{450} = 0.672$.

$$c = A_{450}/\varepsilon_{450} \qquad \textbf{Equation 5.1}$$

From Equation 5.1 it is established that the concentration of the AuNPs solution is 2.52 nM. Despite being a low concentration, even if only one peptide chain was conjugated to one nanoparticle, the peptide concentration would be enough for having biological activity, which is around pmol/cm^2 (Hoyos-Nogués *et al.*, 2017).

✓ The best methodology for obtaining a colloidal 16 nm AuNPs aqueous solution is the 30-minute synthesis following the Turkevich method, as it has been proved by UV-vis spectroscopy and STEM.

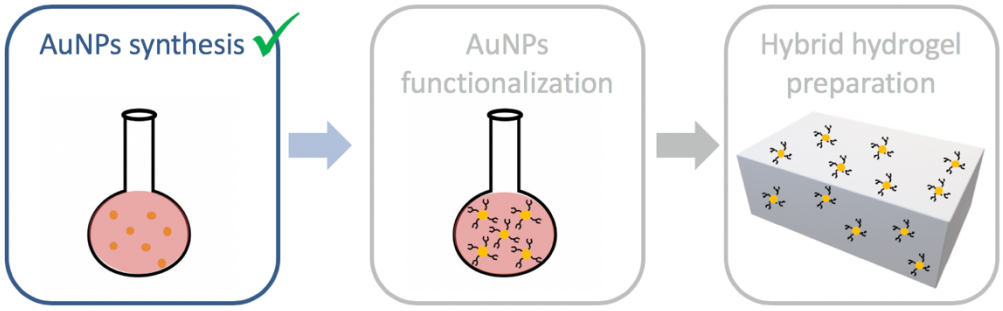

5.2. Characterization of conjugated AuNPs

The AuNPs from the 3rd synthesis were functionalized with linear RGD peptide sequences. The presence of the peptide was determined via UV-Vis spectroscopy (Figure 5.8). A shift in the maximum, compared to the bare AuNPs, is representative of the conjugation (Hosta-Rigau *et al.*, 2010). The peptide conjugation creates a ligand shell around the AuNPs causing an alteration of nanoparticle environment that induces a red-shift of the SPB, because of the different reflection of the light. In the case of thiolate ligands the shift of the SPB is especially important due to the strong interaction between the thiol group and the surface electron cloud of the AuNPs (Astruc and Daniel, 2004).

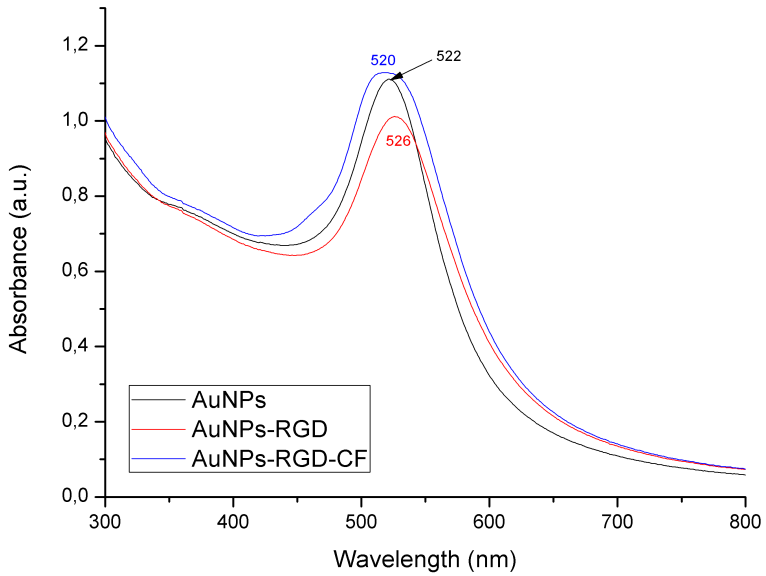

Figure 5.8 UV-vis spectra of bare AuNPs and conjugated AuNPs.

For the AuNPs conjugated with the RGD sequence the shift is towards longer wavelengths (redshift). However, the conjugation with RGD-CF does not have the same behavior. It seems to shift towards lower wavelengths. It could be explained by the fact that carboxyfluorescein (CF) also presents an absorption band around 500 nm, as shown in Figure 5.9, and as a result a wider band appears as a combination of both the AuNPs and the CF.

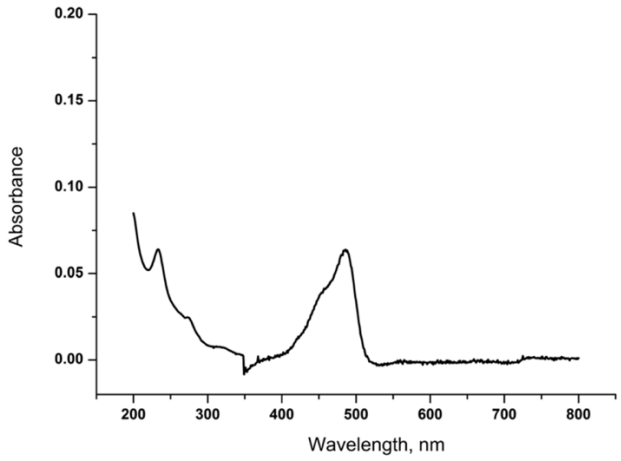

Figure 5.9 UV-vis absorption spectrum of 10 μM fluorescein in water medium, with maximum absorbance observed at 485 nm (Panchompoo *et al.*, 2012).

The peptide sequence modified with a CF tag is used as a marker for fluorescence microscopy. After conjugation and purification via dialysis of the AuNPs, the samples were observed with CLSM. As a control, bare AuNPs were examined and no signal of autofluorescence was detected (Figure 5.10 a). On the contrary, the carboxyfluoresceinated samples emitted a signal that confirmed the presence of peptide attached to the AuNPs (Figure 5.10 b).

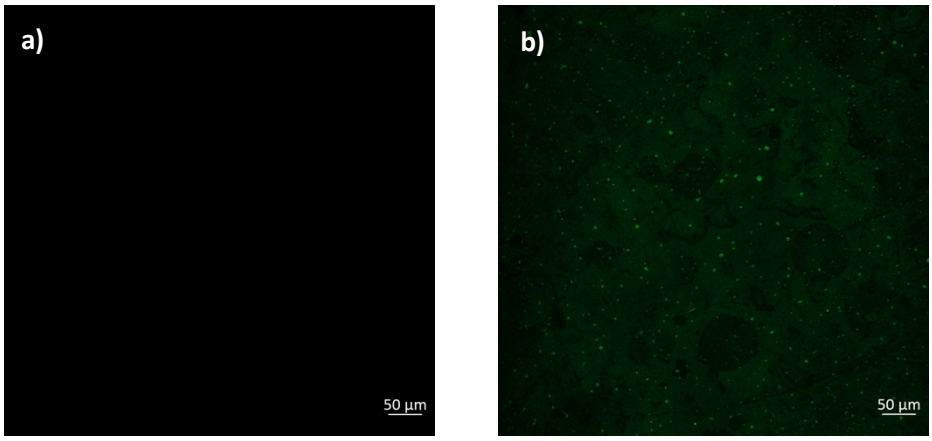

Figure 5.10 CLSM images (a) bare AuNPs and (b) RGD-CF conjugated AuNPs.

✓ The protocol is effective for the functionalization of AuNPs with different peptides having a thiol as the anchoring group.

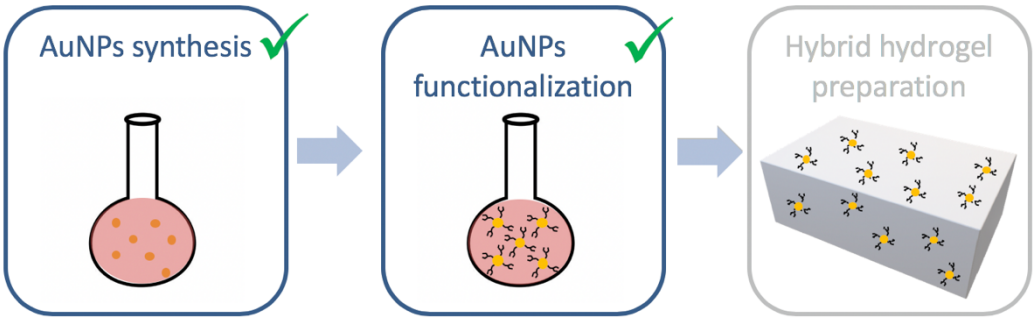

5.3. Characterization of alginate-based films loaded with conjugated AuNPs

Figure 5.11 shows the aspect of the composite hydrogels. Alginate hydrogels are transparent, whereas the loaded hydrogels show a light purple color associated to the presence of the AuNPs. The color is more intense for higher concentrations of AuNPs. The color homogeneity is a first indication of the homogenous distribution of the nanoparticles within the hydrogel.

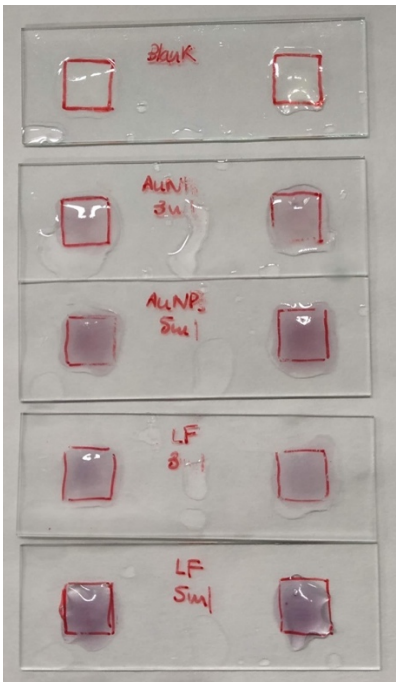

Figure 5.11 Hybrid hydrogels after crosslinking on microscope slides. From top to bottom: alginate, alginate + AuNPs 3mL, alginate + AuNPs 5mL, alginate + AuNPs-LF 3mL and alginate + AuNPs-LF 5mL.

The UV-vis spectra obtained for the dried films is presented in Figure 5.12. As expected, no absorption band is observable for the non-loaded alginate film. The characteristic SPB of AuNPs appears for the rest of samples, but it is shifted towards longer wavelengths with respect to the AuNPs aqueous solution in Figure 5.5 due to the interaction with the alginate network not present in solution. Thus, the presence of AuNPs within the hydrogel matrix is confirmed. On the other hand, the concentration of AuNPs within the hydrogel has also an effect on the intensity of the peak (Heo *et al.*, 2014). As expected, the higher the content is, the higher the intensity is. The trend is observed for the films containing either the functionalized or non-functionalized AuNPs (Alg+AuNPs 3mL, Alg+AuNPs 5mL, Alg+AuNPs-RGD 3mL and Alg+AuNPs-RGD 5mL).

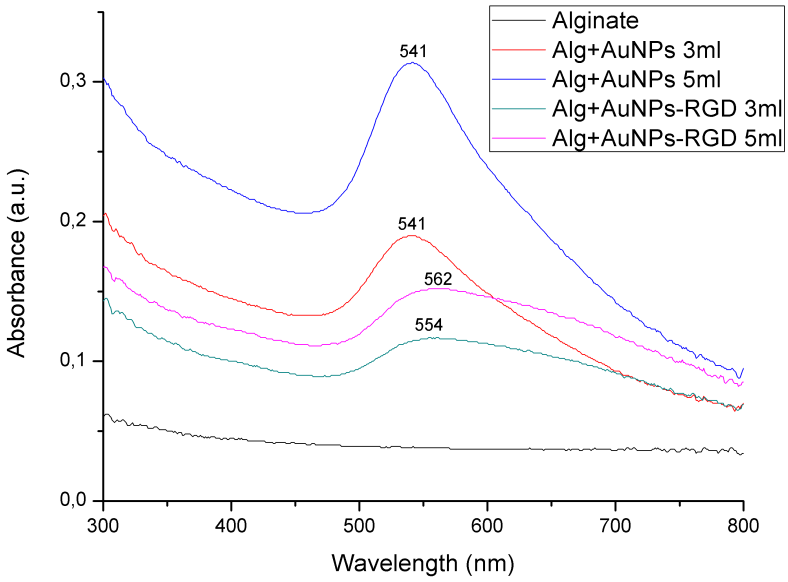

Figure 5.12 UV-vis spectra of alginate-based hydrogel films.

For the purpose of analyzing the AuNPs distribution, STEM images (Figure 5.13 to Figure 5.16) of the carbon-coated films were taken. As foreseen, no AuNPs are present in the control alginate film. Due to the low degradation temperature of the dry alginate film, it was difficult to obtain clear images of the AuNPs as the film was burnt when increasing the intensity of the electron beam. However, the AuNPs could be spotted in all the loaded samples in a brighter color than the background due to the higher atomic number of gold. Bare AuNPs are noticeably more dispersed within the hydrogel matrix in comparison to the conjugated ones. This last ones tend to be more agglomerated in certain regions, probably due to the interaction of the peptide chains.

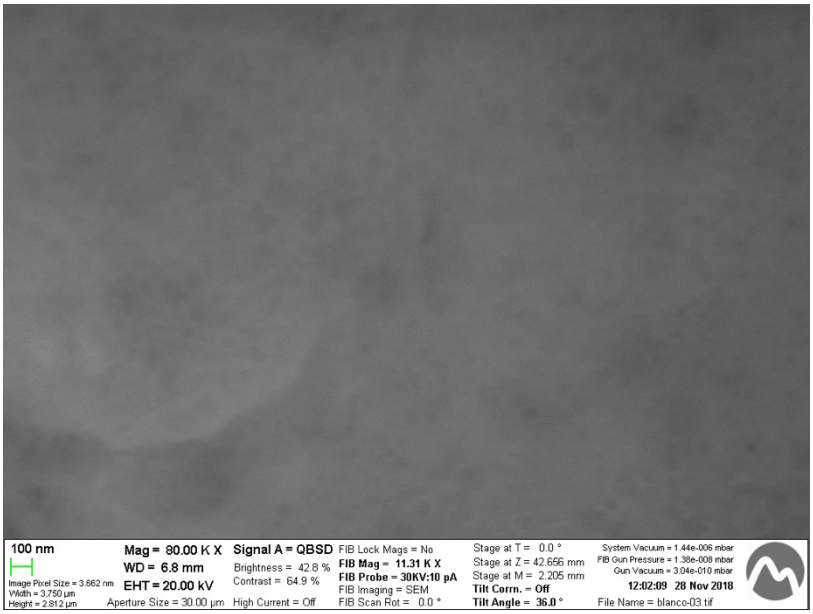

Figure 5.13 STEM image of an alginate film.

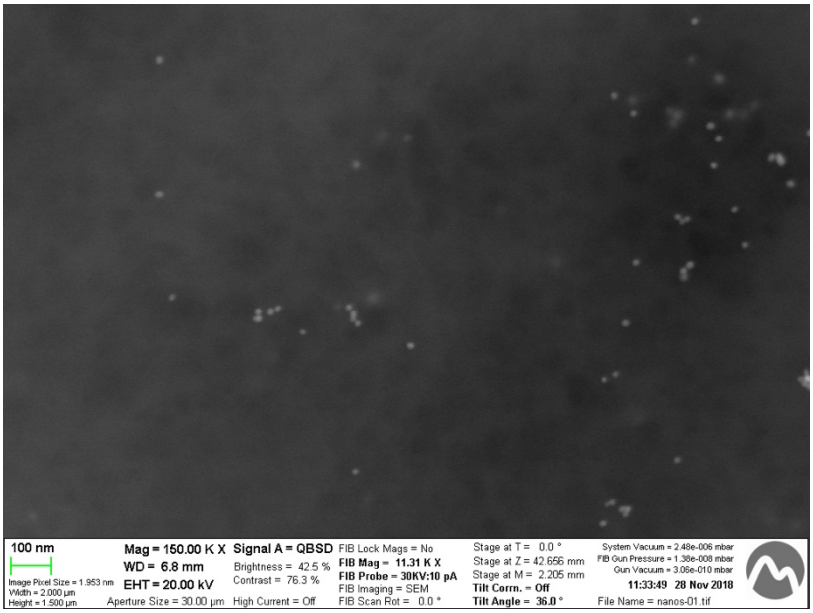

Figure 5.14 STEM image of an alginate film loaded with bare AuNPs.

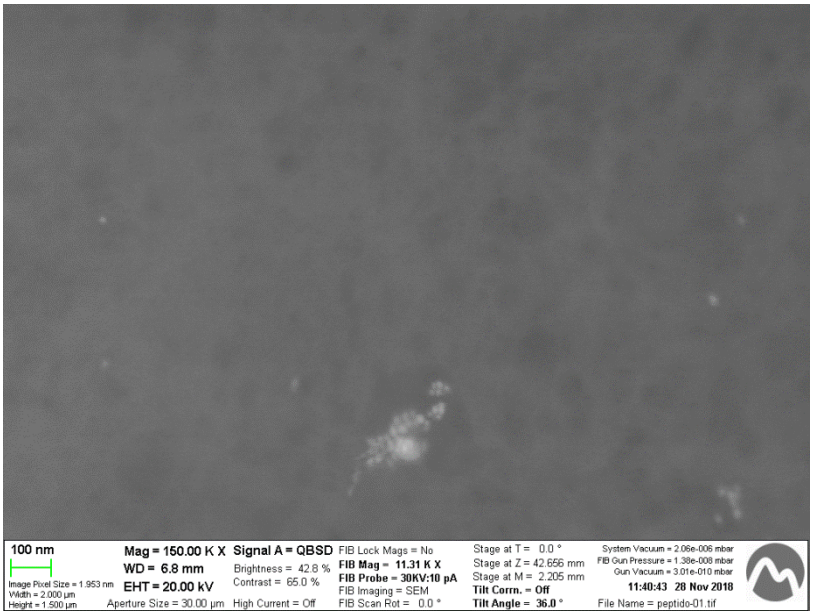

Figure 5.15 STEM image of an alginate film loaded with RGD functionalized AuNPs.

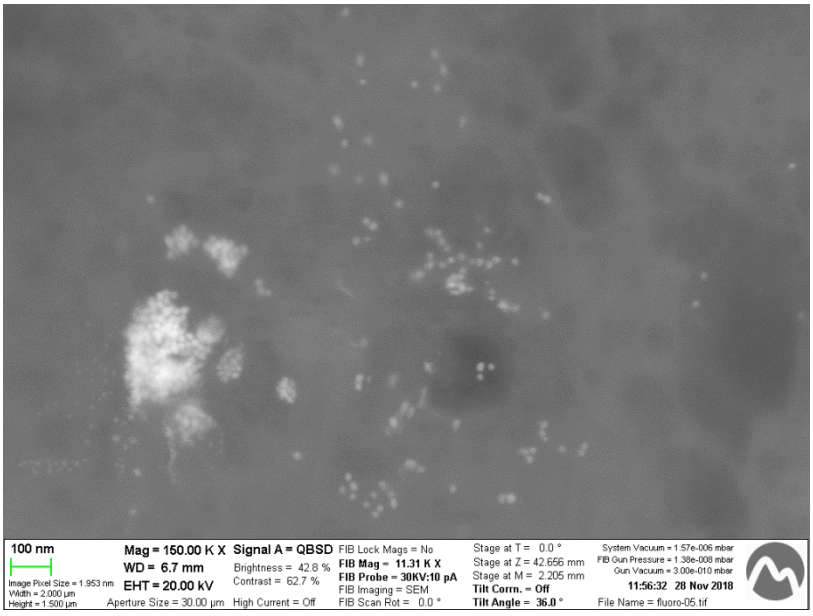

Figure 5.16 STEM image of an alginate film loaded with RGD-CF functionalized AuNPs.

Taking profit of the fluorescence of the conjugated fluorophore, CLSM technique was also used to verify the incorporation of the AuNPs, as shown in Figure 5.17. Some signal is obtained for the alginate film, which is likely to be due to dust particles deposited during the storage or preparation of the samples. In the case of the film loaded with bare AuNPs, no signal was expected either as in Figure 5.10 (a) corresponding to the AuNPs solution. However, some traces can be spotted. The AuNPs solution used for the film preparation is the same as the one characterized in Figure 5.10 (a), corresponding to

the 3rd synthesis of AuNPs. The only difference being that the ones incorporated to the hydrogel were sonicated because of their tendency to agglomerate when stored for several days. Thus, one hypothesis could be contamination coming from the ultrasonic probe. For CF-conjugated AuNPs, omitting the hydrogel dust contamination, a different sort of fluorescent signal is observed surely caused by the carboxyfluoresceinated AuNPs. It is only observed in some regions, certainly due to the uneven distribution of the AuNPs within the film, but it resembles to the one obtained for the conjugated AuNPs solution in Figure 5.10 (b).

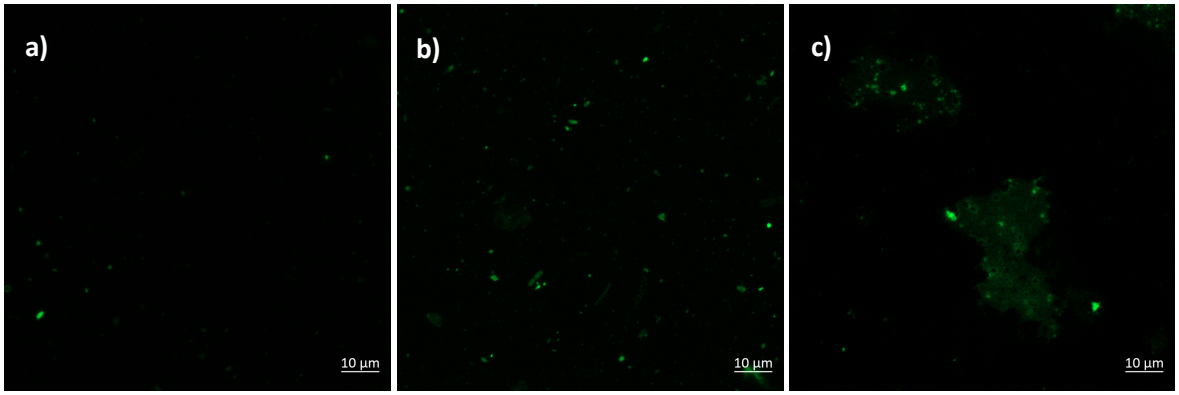

Figure 5.17 CLSM images of hydrogels (a) alginate film, (b) alginate film loaded with bare AuNPs, and (c) alginate film loaded with conjugated AuNPs.

The characterization of the hydrated films via FTIR-ATR does not highlight significant differences among the different samples (Figure 5.18). The spectra of all the dried films only show peaks corresponding to alginate. The band around 3367 cm^{-1} is assigned to hydroxyl groups. The peaks at 1635 and 1419 cm^{-1} correspond to asymmetric and symmetric stretching of carboxyl groups (–COO), respectively. Meanwhile, the band at 1089 cm^{-1} is attributed to C-O stretching vibration and the one at 1033 cm^{-1} to C-O-C stretching mode(Morais *et al.*, 2013). No peaks are assigned to the peptides probably due to its low amount into the hydrogel and undetectable by FTIR.

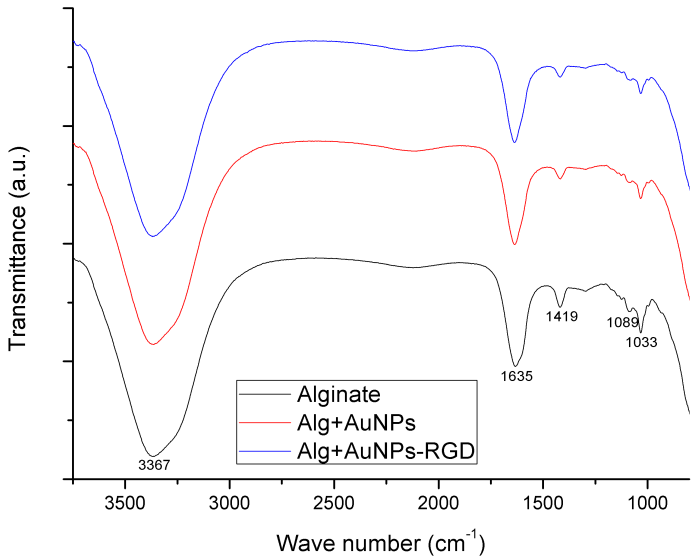

Figure 5.18 FTIR-ATR spectra of alginate films.

The elements analyzed in the XPS assay are C, N, O, S, and Au, as presented in Table 5.1. The most revealing result is the noticeable increase of N in the sample containing the RGD sequence with respect to the other samples. The N content in the samples without peptide might be due to contaminations during the sample manipulation. There is no nitrogen in alginate's chemical composition, but it is present in the amine groups conforming the peptide. The N difference can be attributed to the peptide presence.

Table 5.1 Chemical composition (atomic percentages) measured by XPS.

	C 1s	N 1s	O 1s	S 2p	Au 4f
Alginate	67.59 ± 1.25	0.28 ± 0.03	31.97 ± 1.23	0.17 ± 0.01	0.01 ± 0
Alg+AuNPs	68.35 ± 0.36	0.31 ± 0.08	31.13 ± 0.45	0.21 ± 0.03	0.02 ± 0.01
Alg+AuNPs-RGD	67.47 ± 0.57	0.53 ± 0.08	31.82 ± 0.52	0.18 ± 0.02	0.01 ± 0

On the other hand, no sulfur differences are observed among samples even if it was expected from the thiol group anchoring the peptide to the AuNPs. The proportion of thiol groups with respect to the entire peptide sequence is too small, probably masking their signal.

The atomic percentages of Au do not match the expectations either, as no significant differences are observed among samples, with values in all cases very close to zero. Nevertheless, by direct examination of XPS spectra it is derived that gold is present and actually there are some differences.

Au 4f presents two peaks in the spectra corresponding to Au 4f 5/2 and Au 4f 7/2, as shown in Figure 5.19. Only one of them is visible for the alginate sample, while the two of them are observed for the two other samples containing AuNPs. An unknown element is present in the alginate sample, probably due to a contamination, and it happens to present its binding energy in the same region as Au. This affects the atomic percentages calculations. Moreover, the very low concentration of gold in comparison with the other elements of the samples (e.g. C or O) makes hard to adequate quantify this element by XPS.

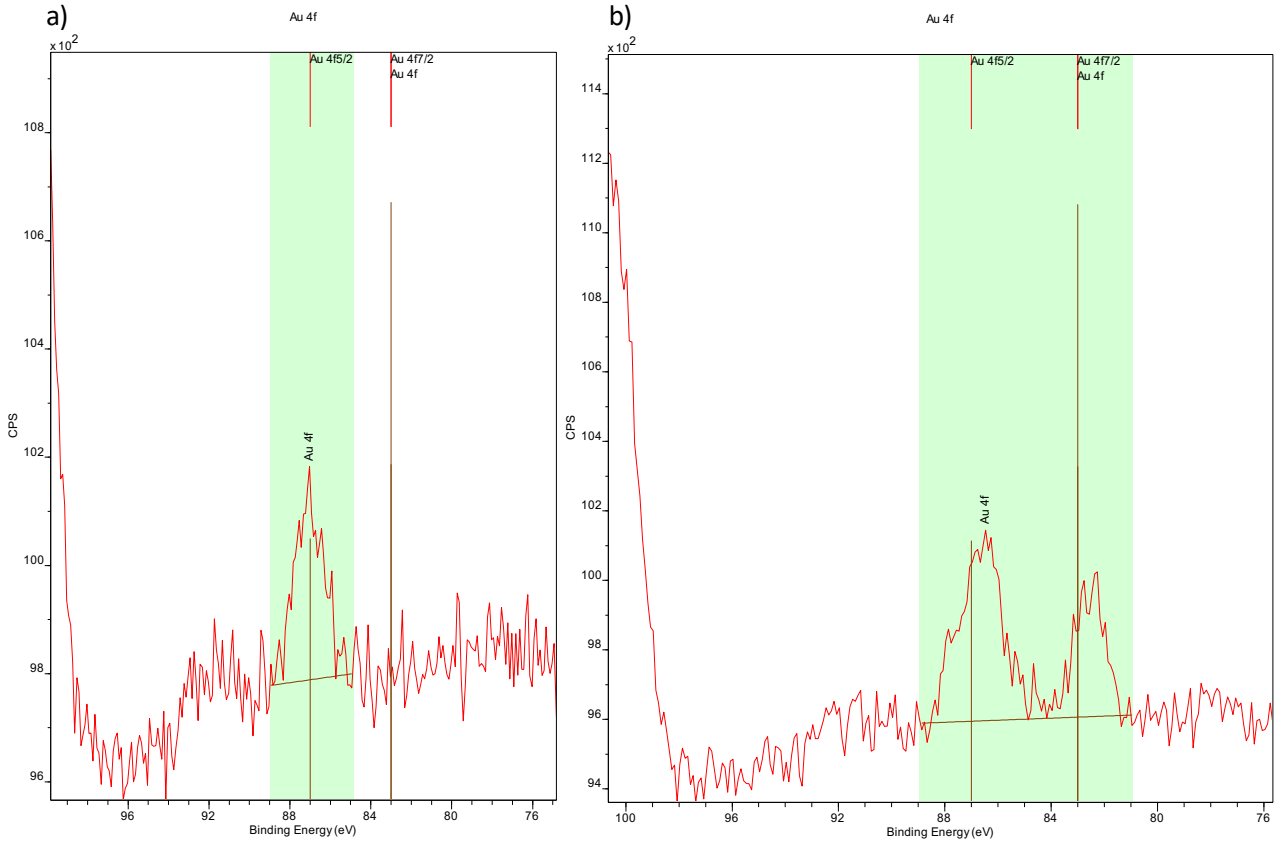

Figure 5.19 XPS results(a) alginate film, and (b) alginate film loaded with AuNPs.

- ✓ Before moving onto the biological characterization, it can be concluded that the final stage of the development of the hybrid hydrogel has been accomplished. The presence of the functionalized AuNPs is guaranteed within the alginate matrix. A methodology has been stablished to prepare plenty of samples with this support.

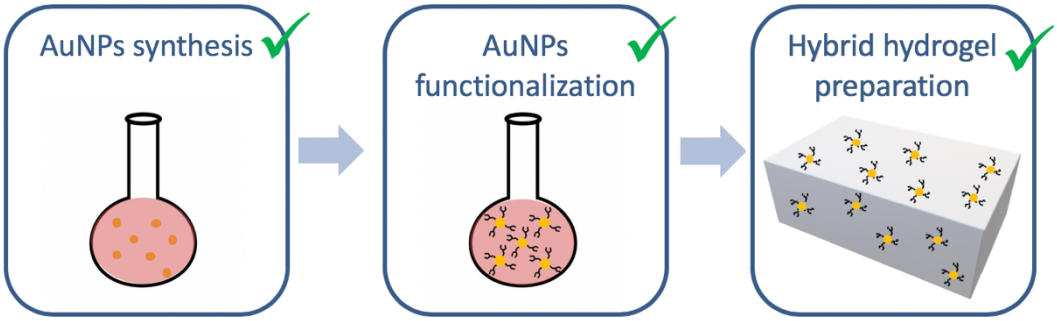

The viability of bacteria was studied with a Live/Dead staining assay using *S. aureus.* From the green and red intensities information of live and dead bacteria can be extracted. The images were taken with CLSM and in Figure 5.20 they are presented as the merge of both green and red channel.

As explained in section 4.6, green stains all bacteria membranes, while red stains only damaged membranes. This implies that when examining the merged images of both channels, dead bacteria should present an orange color resulting from the mix of green and red. This should be the general appearance of the negative control, which was incubated with Triton100 to kill all the bacteria. However, only green-colored bacteria are noticeable. This means that the red signal is not intense enough and we cannot used it as a reference to compare the different samples.

Nevertheless, focusing only on the green staining of all the bacteria attached to the sample some conclusions can be drawn. At first sight, there is no visible reduction of the number of bacteria between the alginate sample and the ones which incorporate AuNPs. However, there is a significant reduction of the bacteria attached to the surface of the samples containing the functionalized AuNPs. Even if there is no red signal showing the dead bacteria, it is already a positive result the decrease in the number of bacteria attached. Two hypotheses could explain this situation, either the LF1-11 prevents bacterial adhesion, either the dead bacteria are no longer attached to the sample due to the several PBS washes during the assay. On the other hand, it can also be extracted that higher concentrations of AuNPs not necessarily increase the antibacterial properties of the hybrid hydrogel.

No concluding results can be determined from this assay since the negative control is not giving the expected results. Further assays should be performed in order to confirm the repeatability of this results.

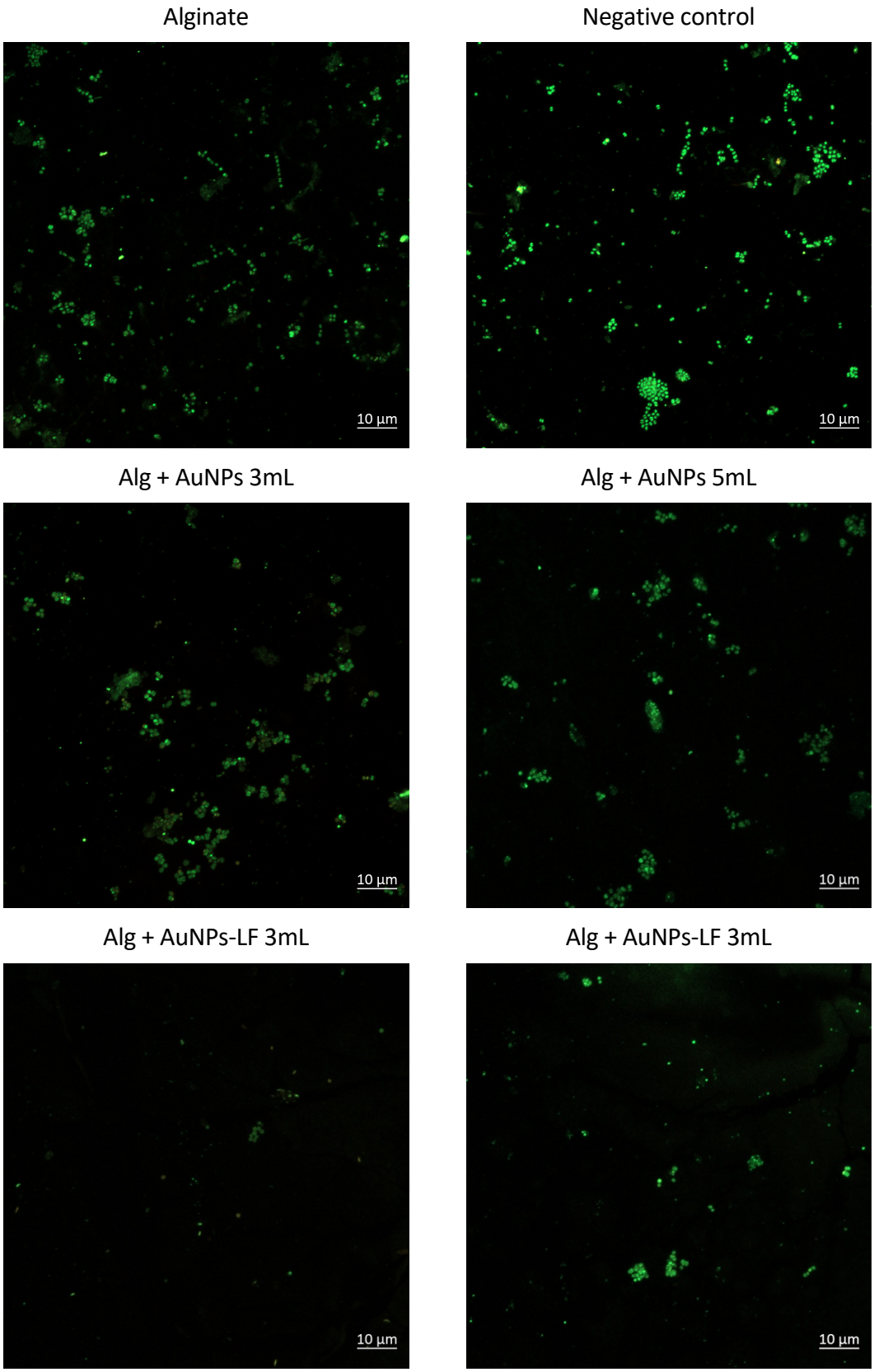

Figure 5.20 Bacterial viability Live/dead assay of *S. aureus.*

6. Achievements and work perspective

A methodology has been stablished for the production of alginate-based hydrogels loaded with functionalized AuNPs. Involving the synthesis of AuNPS, their peptide functionalization and the final fabrication of the hybrid hydrogel.

Apparently, there is a noticeable reduction of the number of bacteria in the LF1-11-functionalized hydrogels. However, further bioactivity assays to test the response of bacteria and eukaryotic cells to this novel biomaterial will be required. Bacterial assays with the linear LF1-11 sequence, cell culture assays with the linear RGD sequence and, ultimately, assays with the multifunctional peptide platform.

Improving the homogeneous distribution of the AuNPs within the hydrogel matrix would be an asset too in order to have a more representative response during the assays.

7. Environmental impact

Nowadays, when developing a new product, its environmental impact has to be imperatively analyzed. In this project, a few reagents which could have an environmental impact were used. All the residues issued from our experiences were carefully recycled or selectively sorted in order to respect specific normative, especially for dangerous products. All the laboratories where experimental tasks are carried out are subjected to strict residue management. Chemical residues are collected in specific labeled containers and all contaminated disposable material is thrown in a special container to be treated by a specialized company.

Another environmentally friendly strategy was prioritizing the use of glass in the laboratory, which has unlimited use, and reusing the plastic containers as many times as possible to minimize the waste.

Conclusion

Throughout this project a novel composite biomaterial has been developed. A hybrid hydrogel containing peptide-functionalized gold nanoparticles (AuNPs) has been conceived for potential applications as a novel biomaterial in the field of regenerative medicine. The functionalization not only promotes cell adhesion, but also provides the biomaterial with antibacterial properties, a major concern for medical devices.

Due to the composite nature of the biomaterial, the process was divided into three stages: AuNPs synthesis, AuNPs functionalization, and film preparation. Each step was successfully accomplished and validated by different characterization techniques.

AuNPs synthesis, following the Turkevich method, can be considered a highly reproducible process. The methodology, previously unknown by the research group, has been established and different parameters optimized. To deal with AuNPs tendency to agglomerate over time, probe sonication was required before employing them. Two types of peptides, RGD and LF1-11, were efficiently conjugated to the AuNPs, thus thiol seems to be an appropriate anchoring group for gold substrates. UV-vis spectroscopy turned out to be the simplest, yet consistent technique for verifying the AuNPs synthesis and the peptide conjugation, thanks to the optical properties of AuNPs.

As for the hybrid hydrogel preparation, a method has also been established controlling key parameters such as alginate's composition or crosslinking time. Regarding the biological characterization, no concluding results can be assigned to the biomaterial performance. The hybrid hydrogel functionalized with LF1-11 seems to reduce the number of bacteria to a considerable extent. Further studies with bacteria and eukaryotic cells could shed light to the potential applications of this hybrid system in the clinical setting.

Economic analysis

An analysis of all the resources used for the development of the current project is detailed in the tables below. Main expenses come from staff and the characterization techniques used during the project. The estimate cost of this 5-month project is around 6,500€.

Table 0.1 AunNPs synthesis

Product	**Quantity**	**Price**	**Cost (€)**
MQ Water	330 mL	90€/1.5L	19.80
Sample container 150 mL	5	50€/350 units	0.71
Sodium citrate	300 mg	42.90€/Kg	0.01
Tetrachloroauric acid	30 mg	169€/500mg	10.14
Tip 5 mL	6	66.17€/960 units	0.41
			31.08

Table 0.2 Peptide conjugation

Product	**Quantity**	**Price**	**Cost (€)**
Dialysis membrane	1 m	132.30€/30m	4.41
Distilled Water	9 L	0.60€/L	5.40
LF1-11	1 mg	100€/mg	100.00
RGD	4 mg	100€/mg	400.00
Sodium citrate	2.34 g	42.90€/Kg	0.10
Tip 1 mL	5	54.17€/960 units	0.28
Tip 5 mL	5	66.17€/960 units	0.34
			510.54

Table 0.3 Film preparation

Product	**Quantity**	**Price**	**Cost (€)**
Alginic acid sodium salt	3 g	31.40€/250g	0.38
Calcium chloride	30 g	112€/100g	33.60
Distilled Water	3.5 L	0.60€/L	2.10
Falcon 15 mL	10	200€/500 units	4.00
Pasteur pipette 3 mL	20	23.30€/500 units	0.93
Sample container 40 mL	10	160€/800 units	2.00
			43.01

Table 0.4 Bacterial assays

Product	**Quantity**	**Price**	**Cost (€)**
24-well plate	6	65€/5 plates	78.00
BHI powder	37 g	36,.0€/100g	13.47
Falcon 15 mL	4	200€/500 units	1.60
PBS	1 tablet	168€/100 tablets	1.68
Tip 1 mL	20	54.17€/960 units	1.13
Tip 200uL	20	59.28€/960 units	1.24
Ethanol	1 L	25.50€/L	25.50
Sample container 40 mL	10	160€/800 units	2.00
Glutaraldehyde solution	2 mL	36.10/100mL	0.72
LIVE/DEAD™ BacLight™ Bacterial Viability Kit	8 μL	612€/600 μL	8.16
			133.49

Table 0.5 Characterization techniques

Technique	**Quantity (h)**	**Price (€/h)**	**Cost (€)**
Carbon coating	0.25	20	5
CLSM	10	30	300
FTIR	2	5	10
SEM	4	110	440
TEM	2	110	220
UV-vis	7	5	35
XPS	6	80	480
			1490

Table 0.6 Staff

Position	**Quantity (h)**	**Price (€/h)**	**Cost (€)**
Project director	60	60	3600
Technician	20	31	620
Master student	720	-	-
			4220

References

Astruc, D. and Daniel, M.-C. (2004) 'Gold Nanoparticles: Assembly, Supramolecular Chemistry, Quantum-Size-Related Properties, and Applications toward Biology, Catalysis, and Nanotechnology', *Chemical Reviews*, 104(1), pp. 293–346. Available at: http://pubs3.acs.org/acs/journals/doilookup?in_doi=10.1021/cr030698+%5Cnhttp://pubs.acs.org/cgi-bin/article.cgi/chreay/2004/104/i01/pdf/cr030698+.pdf?sessid=%5Cnhttp://pubs.acs.org/error.html.

Augst, A. D., Kong, H. J. and Mooney, D. J. (2006) 'Alginate hydrogels as biomaterials', *Macromolecular Bioscience*, 6(8), pp. 623–633. doi: 10.1002/mabi.200600069.

Avvakumova, S. *et al.* (2014) 'Development of U11-functionalized gold nanoparticles for selective targeting of urokinase plasminogen activator receptor-positive breast cancer cells', *Bioconjugate Chemistry*, 25(8), pp. 1381–1386. doi: 10.1021/bc500202b.

Bidarra, S. J., Barrias, C. C. and Granja, P. L. (2014) 'Injectable alginate hydrogels for cell delivery in tissue engineering', *Acta Biomaterialia*, 10(4), pp. 1646–1662. doi: 10.1016/j.actbio.2013.12.006.

Caliari, S. R. and Burdick, J. A. (2016) 'A practical guide to hydrogels for cell culture', *Nature Methods*. Nature Publishing Group, 13(5), pp. 405–414. doi: 10.1038/nmeth.3839.

Caló, E. and Khutoryanskiy, V. V. (2015) 'Biomedical applications of hydrogels: A review of patents and commercial products', *European Polymer Journal*, 65, pp. 252–267. doi: 10.1016/j.eurpolymj.2014.11.024.

Drabczyk, A. *et al.* (2017) 'Colloids and Surfaces B : Biointerfaces Preparation and cytotoxicity of chitosan-based hydrogels modified with silver nanoparticles', 160, pp. 325–330. doi: 10.1016/j.colsurfb.2017.09.044.

González-Sánchez, M. I. *et al.* (2015) 'Silver nanoparticle based antibacterial methacrylate hydrogels potential for bone graft applications', *Materials Science and Engineering C*. Elsevier B.V., 50, pp. 332–340. doi: 10.1016/j.msec.2015.02.002.

Haiss, W. (2007) 'Determination of size and concentration of gold nanoparticles from extinction spectra', *Analytical chemistry*, 79(17), pp. 6215–4221. doi: 10.1007/s00216-007-1768-z.

Heo, D. N. *et al.* (2014) 'Enhanced bone regeneration with a gold nanoparticle-hydrogel complex', *Journal of Materials Chemistry B*, 2(11), pp. 1584–1593. doi: 10.1039/c3tb21246g.

Hosta-Rigau, L. *et al.* (2010) 'Multifunctionalized gold nanoparticles with peptides targeted to gastrin-releasing peptide receptor of a tumor cell line', *Bioconjugate Chemistry*, 21(6), pp. 1070–1078. doi: 10.1021/bc1000164.

Hosta, L. *et al.* (2009) 'Conjugation of Kahalalide F with gold nanoparticles to enhance in vitro antitumoral activity', *Bioconjugate Chemistry*, 20(1), pp. 138–146. doi: 10.1021/bc800362j.

Hoyos-Nogués, M. *et al.* (2017) 'Regenerating Bone via Multifunctional Coatings: The Blending of Cell

Integration and Bacterial Inhibition Properties on the Surface of Biomaterials', *ACS Applied Materials and Interfaces*, 9(26), pp. 21618–21630. doi: 10.1021/acsami.7b03127.

Hoyos-Nogués, M. *et al.* (2018) 'All-in-one trifunctional strategy: A cell adhesive, bacteriostatic and bactericidal coating for titanium implants', *Colloids and Surfaces B: Biointerfaces*. Elsevier B.V., 169, pp. 30–40. doi: 10.1016/j.colsurfb.2018.04.050.

Hunt, J. A. *et al.* (2014) 'Hydrogels for tissue engineering and regenerative medicine', *Journal of Materials Chemistry B*. Royal Society of Chemistry, 2(33), pp. 5319–5338. doi: 10.1039/c4tb00775a.

Kogan, M. J. *et al.* (2007) 'Peptides and metallic nanoparticles for biomedical applications', *Nanomedicine*, 2(3), pp. 287–306. doi: 10.2217/17435889.2.3.287.

Marsich, E. *et al.* (2011) 'Biological response of hydrogels embedding gold nanoparticles', *Colloids and Surfaces B: Biointerfaces*. Elsevier B.V., 83(2), pp. 331–339. doi: 10.1016/j.colsurfb.2010.12.002.

Mei, S. *et al.* (2014) 'Antibacterial effects and biocompatibility of titanium surfaces with graded silver incorporation in titania nanotubes', *Biomaterials*, 35(14), pp. 4255–4265. doi: 10.1016/j.biomaterials.2014.02.005.

Morais, D. S. *et al.* (2013) 'Development and characterization of novel alginate-based hydrogels as vehicles for bone substitutes', *Carbohydrate Polymers*. Elsevier Ltd., 95(1), pp. 134–142. doi: 10.1016/j.carbpol.2013.02.067.

Murphy, C. J. *et al.* (2008) 'Chemical sensing and imaging with metallic nanorods', *Chemical Communications*, 8(5), pp. 544–557. doi: 10.1039/b711069c.

Panchompoo, J. *et al.* (2012) 'One-step synthesis of fluorescein modified nano-carbon for Pd(ii) detection via fluorescence quenching', *Analyst*, 137(9), pp. 2054–2062. doi: 10.1039/c2an16261j.

Pereira, L., Gheda, S. F. and Ribeiro-Claro, P. J. A. (2013) 'Analysis by Vibrational Spectroscopy of Seaweed Polysaccharides with Potential Use in Food, Pharmaceutical, and Cosmetic Industries', *International Journal of Carbohydrate Chemistry*, 2013(vi), pp. 1–7. doi: 10.1155/2013/537202.

Sonavane, G., Tomoda, K. and Makino, K. (2008) 'Biodistribution of colloidal gold nanoparticles after intravenous administration: Effect of particle size', *Colloids and Surfaces B: Biointerfaces*, 66(2), pp. 274–280. doi: 10.1016/j.colsurfb.2008.07.004.

Wuithschick, M. *et al.* (2015) 'Turkevich in New Robes: Key Questions Answered for the Most Common Gold Nanoparticle Synthesis', *ACS Nano*, 9(7), pp. 7052–7071. doi: 10.1021/acsnano.5b01579.

Yeh, Y. C., Creran, B. and Rotello, V. M. (2012) 'Gold nanoparticles: Preparation, properties, and applications in bionanotechnology', *Nanoscale*, 4(6), pp. 1871–1880. doi: 10.1039/c1nr11188d.

Zhao, P., Li, N. and Astruc, D. (2013) 'State of the art in gold nanoparticle synthesis', *Coordination Chemistry Reviews*, 257(3–4), pp. 638–665. doi: 10.1016/j.ccr.2012.09.002.